

Elastography, tribo elastography and passive elastography

Stefan Catheline

University of Paris 7, LOA (Institut Langevin), M.Fink

University of Montevideo (Uruguay) LAU, C. Negreira

University of Grenoble, ISTerre, M.Campillo

University of Lyon, INSERM, LabTAU, J-Y Chapelon

Part I: Overview of elastography



Reflection coefficient $R_a = \frac{Z_2 - Z_1}{Z_2 + Z_1}$

Impedance $Z = \rho C = \sqrt{\rho(\lambda + 2\mu)}$



Ultrasound devices give impedance variation imaging

Years

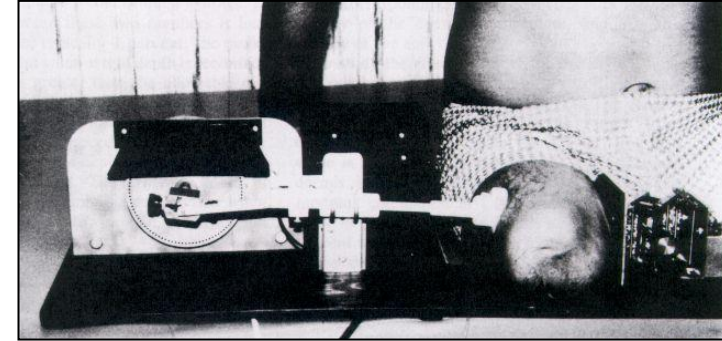
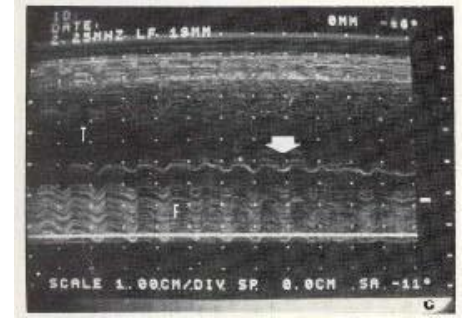
Qualitatif

1981 Natural motion (Dickinson)

1983 Vibrator (Eisencher Echosisomography)

Quantitatif

1987 **Monochromatic** + Doppler (Krouskop)



Elastic, homogeneous,
isotropic, linear

$$(\lambda + 2\mu) \overrightarrow{\text{grad}} \text{div}(\vec{u}) - \mu \overrightarrow{\text{rot}} \overrightarrow{\text{rot}} \vec{u} - \rho \frac{\partial^2 \vec{u}}{\partial t^2} = \vec{0}$$

$$C_P = \sqrt{\frac{\lambda + 2\mu}{\rho}} \approx \sqrt{\frac{\lambda}{\rho}}$$

$$C_S = \sqrt{\frac{\mu}{\rho}}$$

Soft tissues:

$$\lambda = 2,5 \text{ Gpa}$$

$$\mu = 25 \text{ kPa} \ll \lambda$$

Water and soft tissues are incompressible

Manual palpation reveals shear elasticity μ

Shear waves are slow.

Years

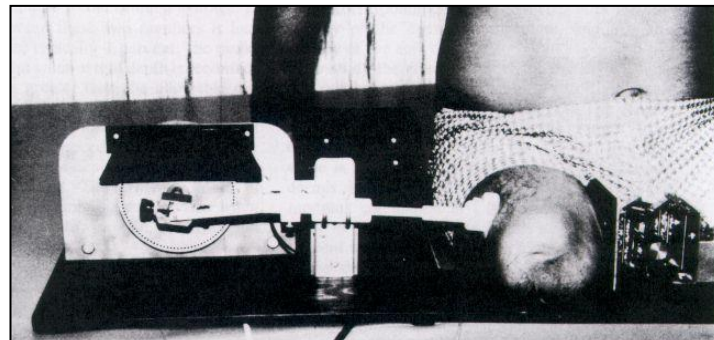
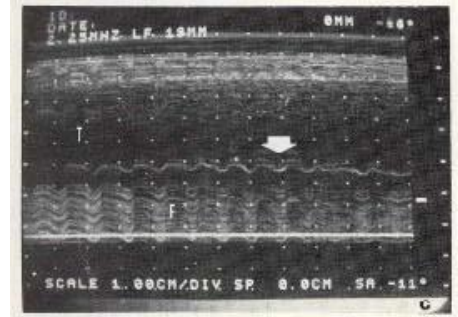
Qualitatif

1981 Natural motion (Dickinson)

1983 Vibrator (Eisencher Echosisomography)

Quantitatif

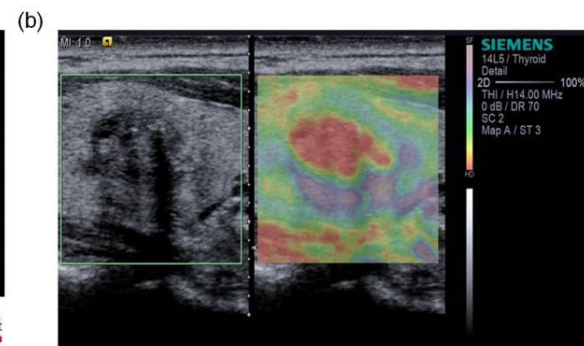
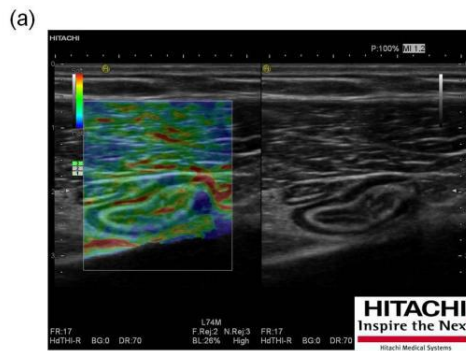
1987: **Monochromatic** + Doppler (Krouskop)



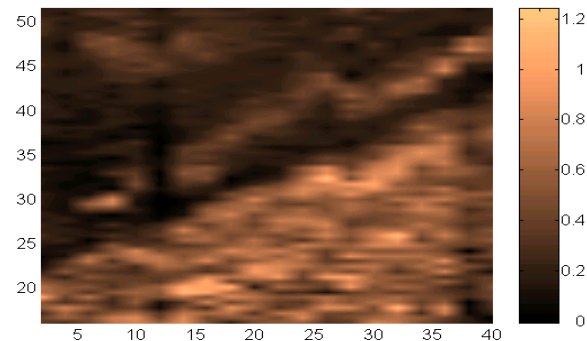
1991: **Static** (Ophir)

Hooke's law:

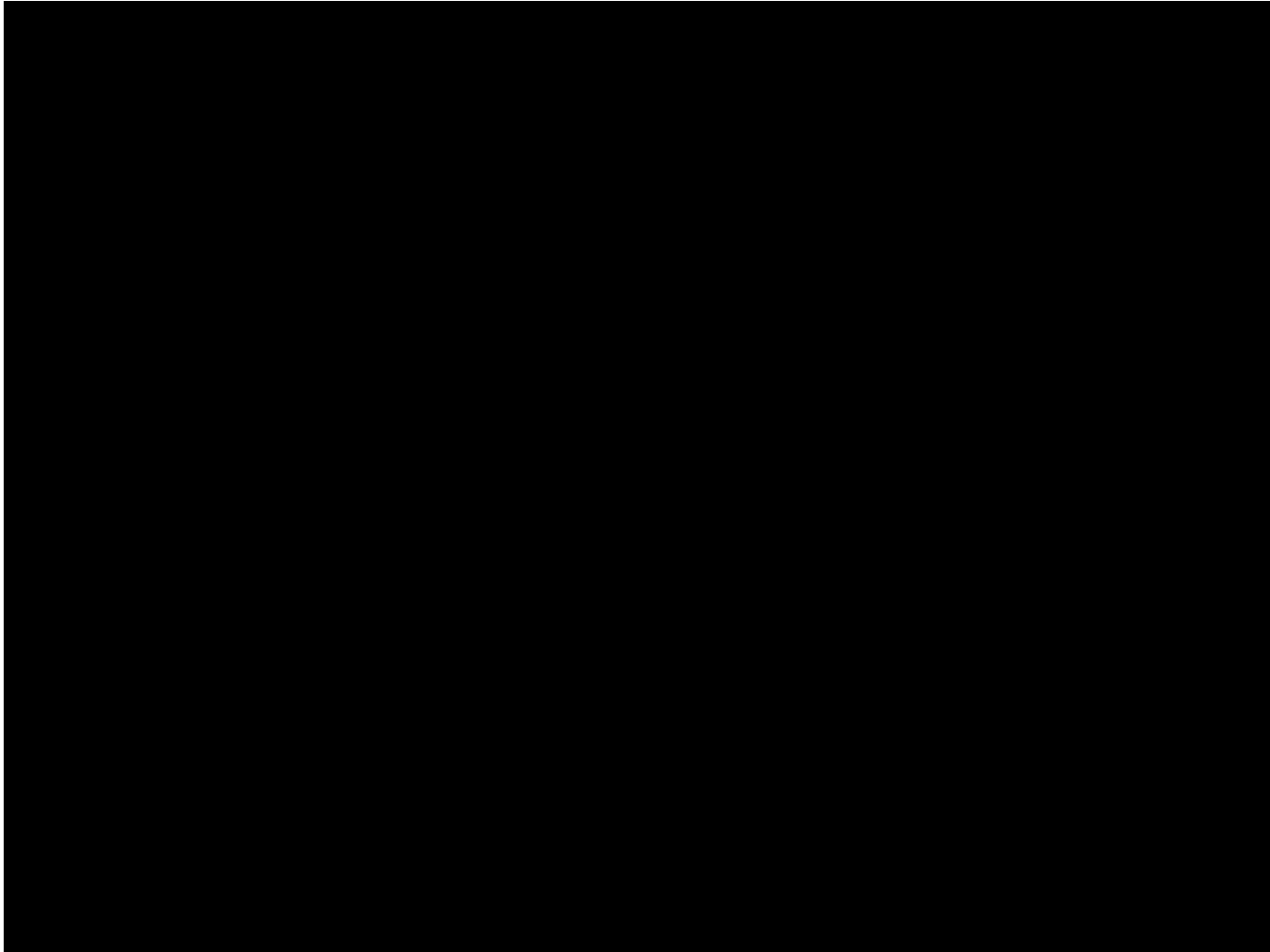
$$T_{ij} = C_{ijkl} S_{kl}$$



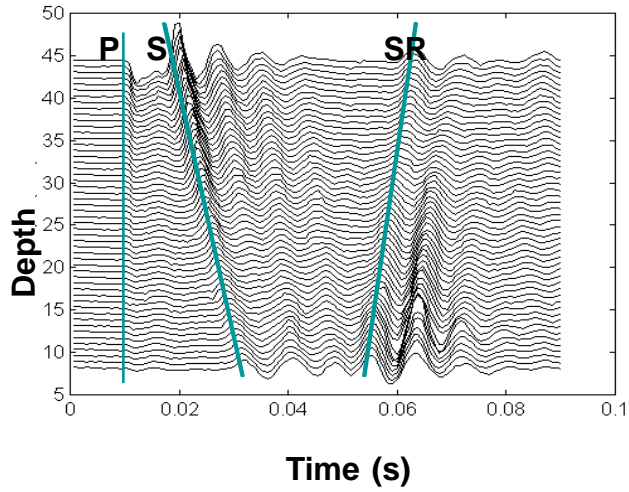
1998: **Pulse** (Fink, Catheline)



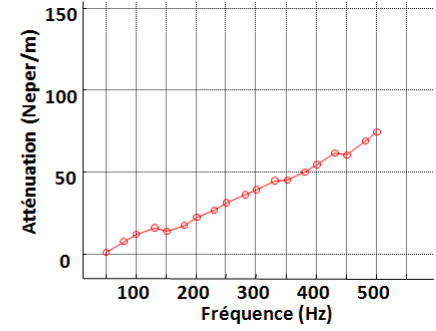
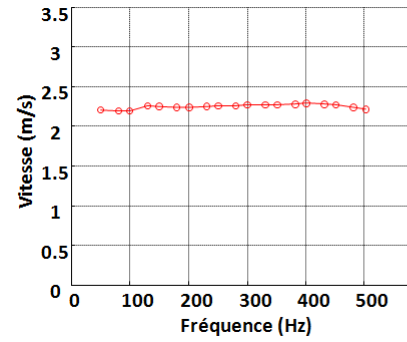
I Elastography



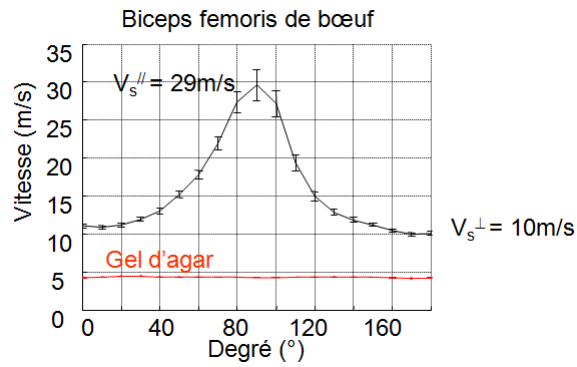
Elastodynamic



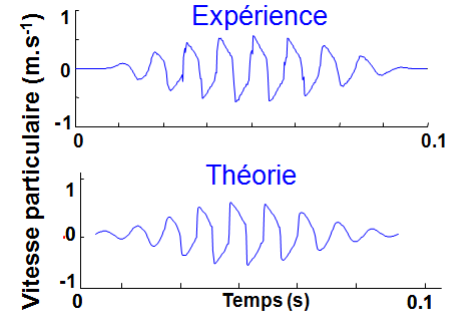
Rheology



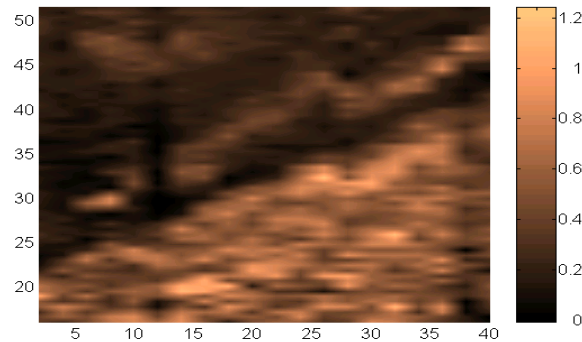
Anisotropy



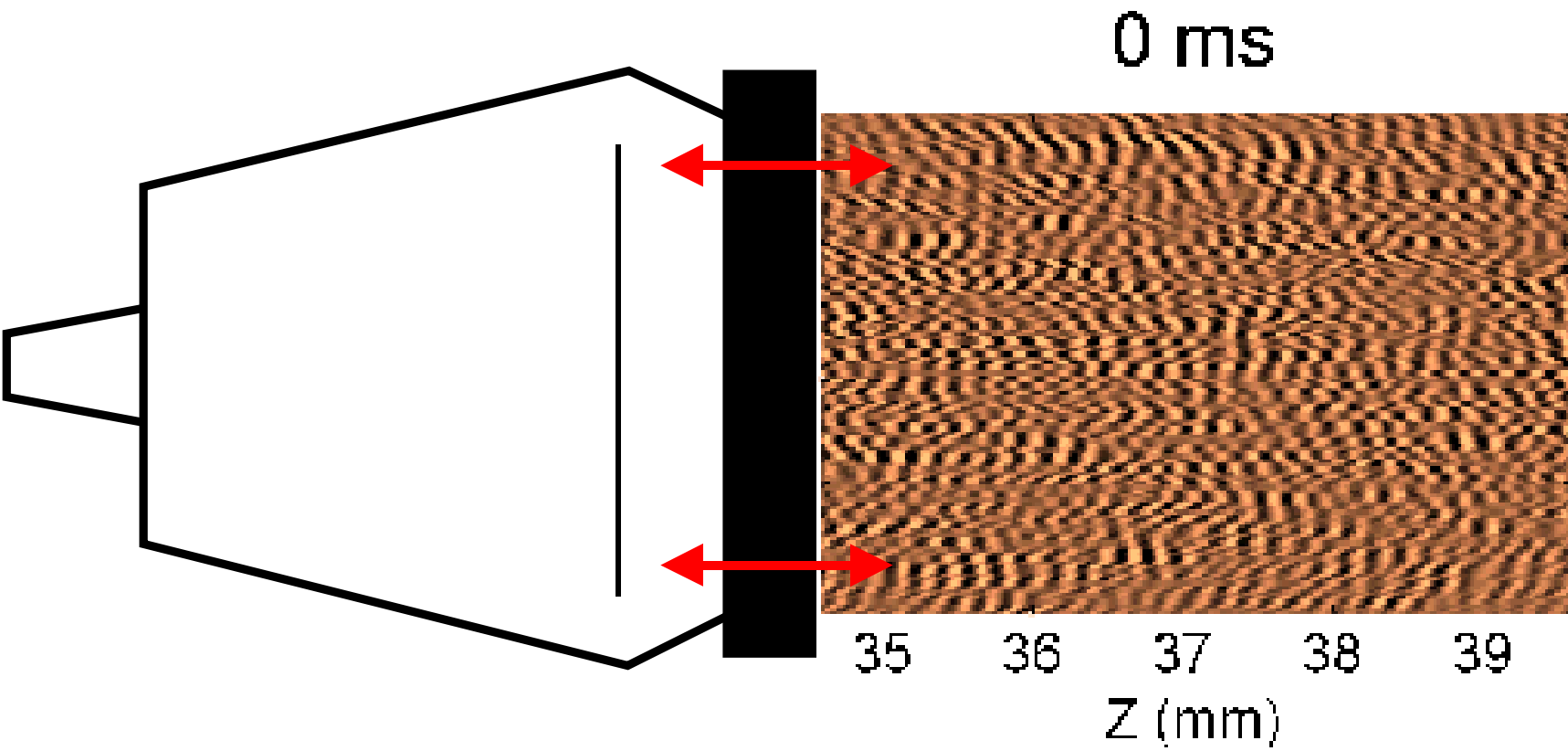
Non linearity



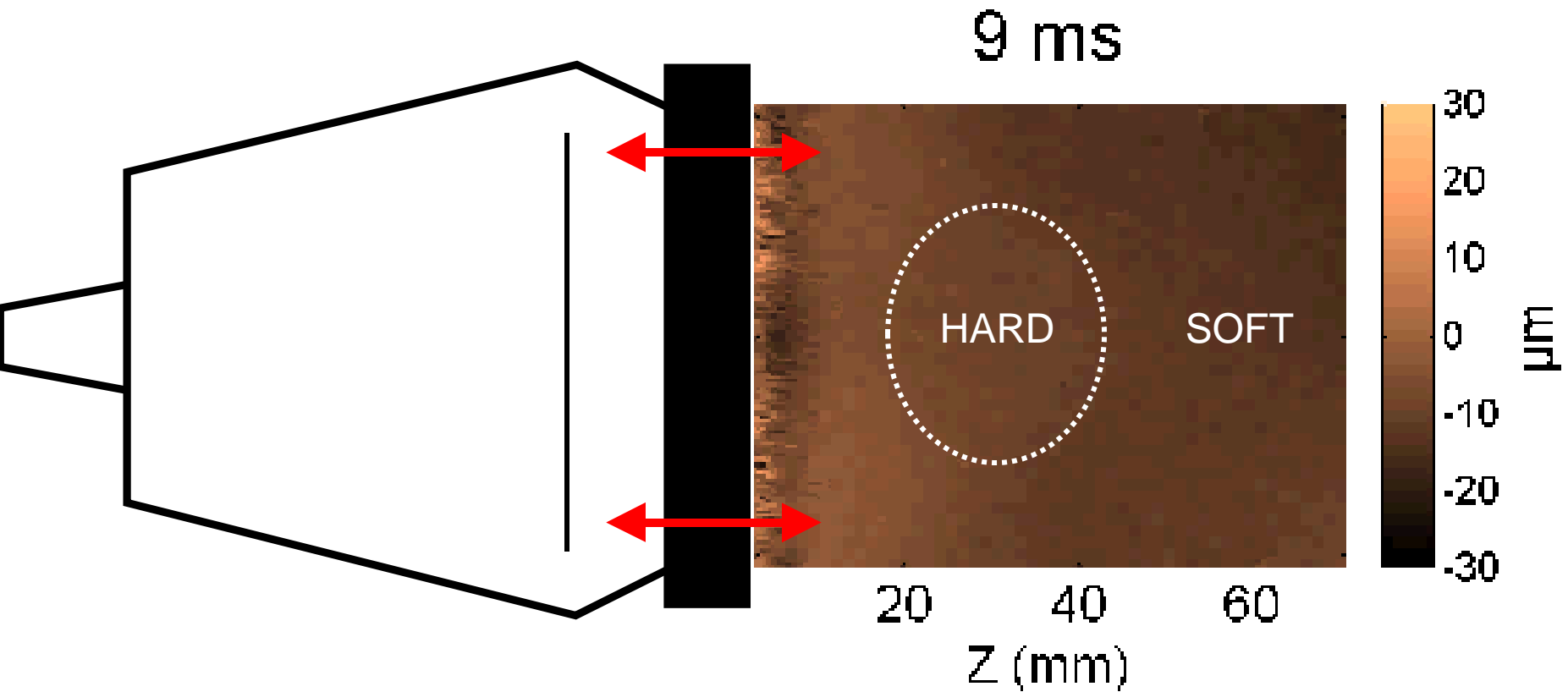
Imaging



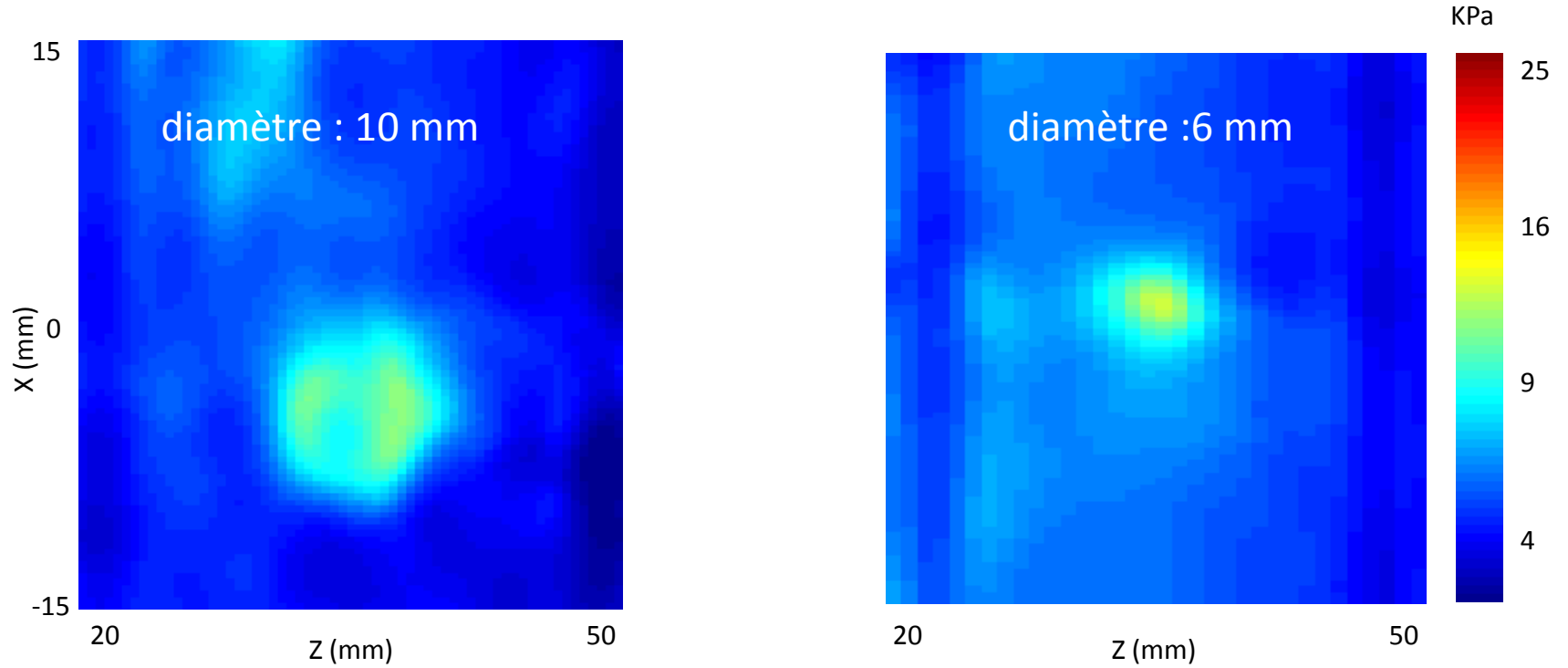
Ultrasound speckle interferometry



Experimental movie of the z component of the displacements



Example of inclusions in gels



Years

Qualitatif

1981 Natural motion (Dickinson)

1983 Vibrator (Eisencher Echosismography)

Quantitatif

1987: **Monochromatic** + Doppler (Krouskop)

1990: **Monochromatic** + Doppler (Levinson, Parker, Sato)

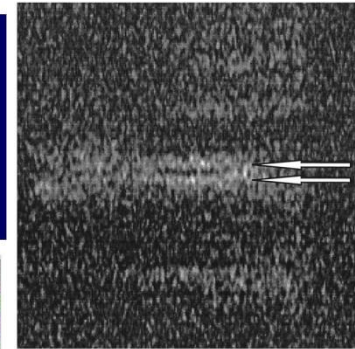
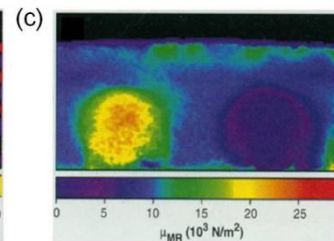
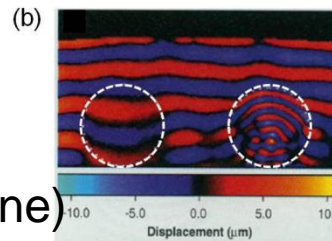
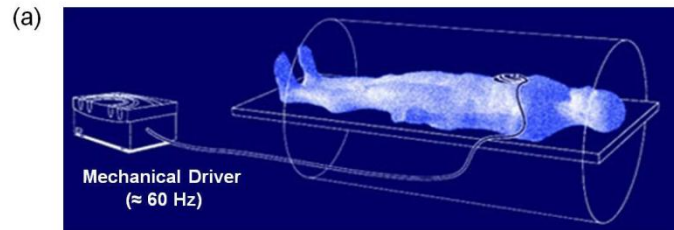
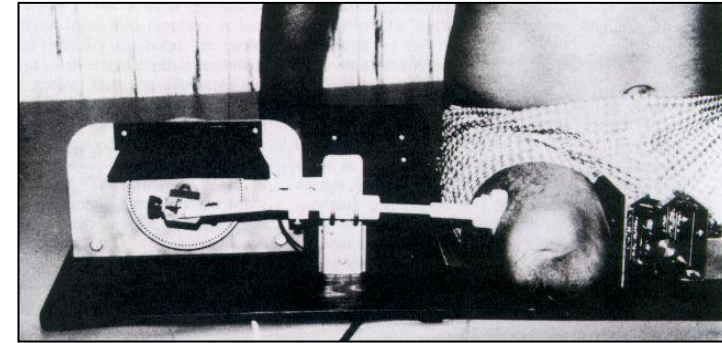
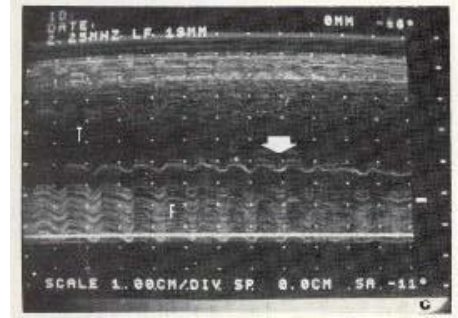
1991: **Static** +Ultrasound (Ophir)

1995: **Monochromatic**+MRI (Greenleaf)

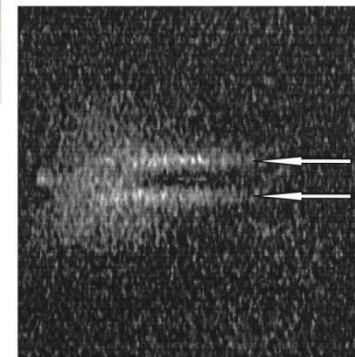
1998: **Pulse**+ultrasound (Fink, Catheline)

1998: **Pulse**+MRI+Radiation pressure (Sarvazian)

2004: **Pulse**+ultrasound (Fink, Tanter, Bercoff)

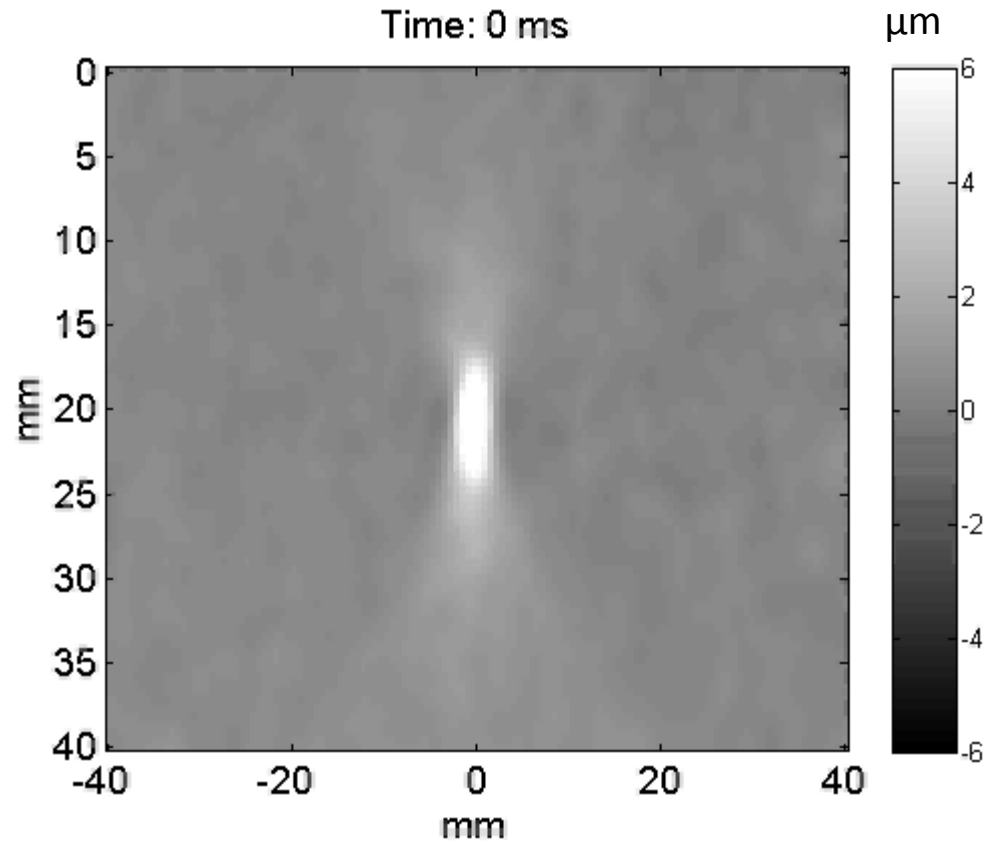
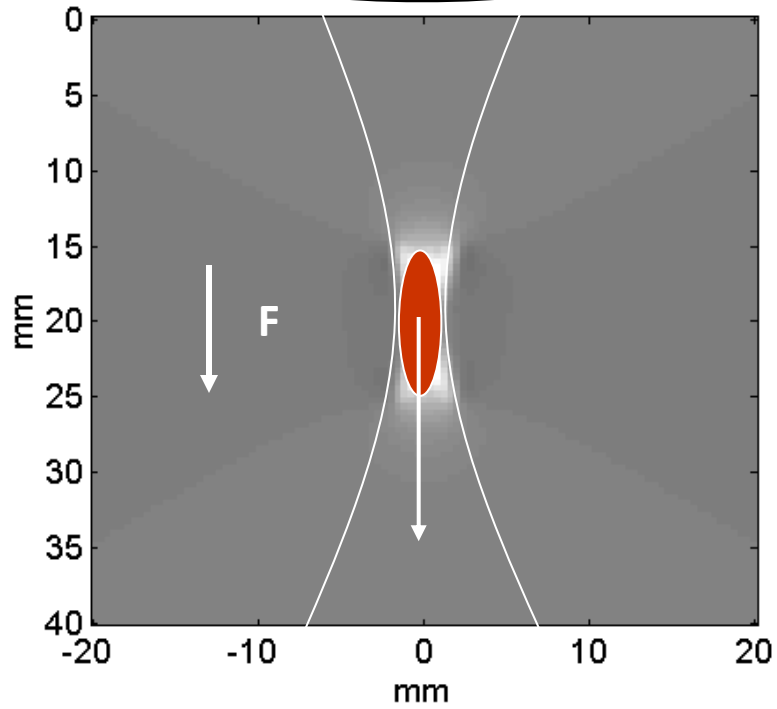
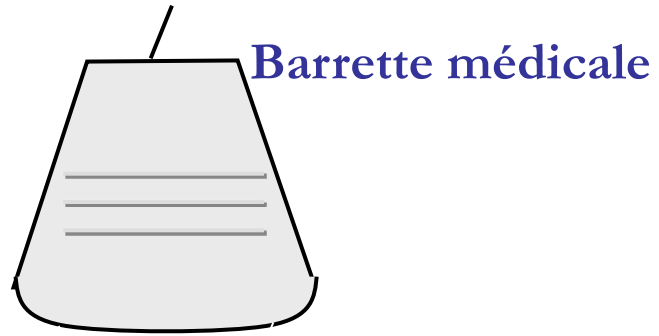


(a)



(b)

La pression de radiation



Echosens (2003): le Fibroscan



Supersonic Imagine (2008): l'Aixplorer



Part II: From Medical Imaging to seismology

-Sliding dynamic studies by use of elastography-

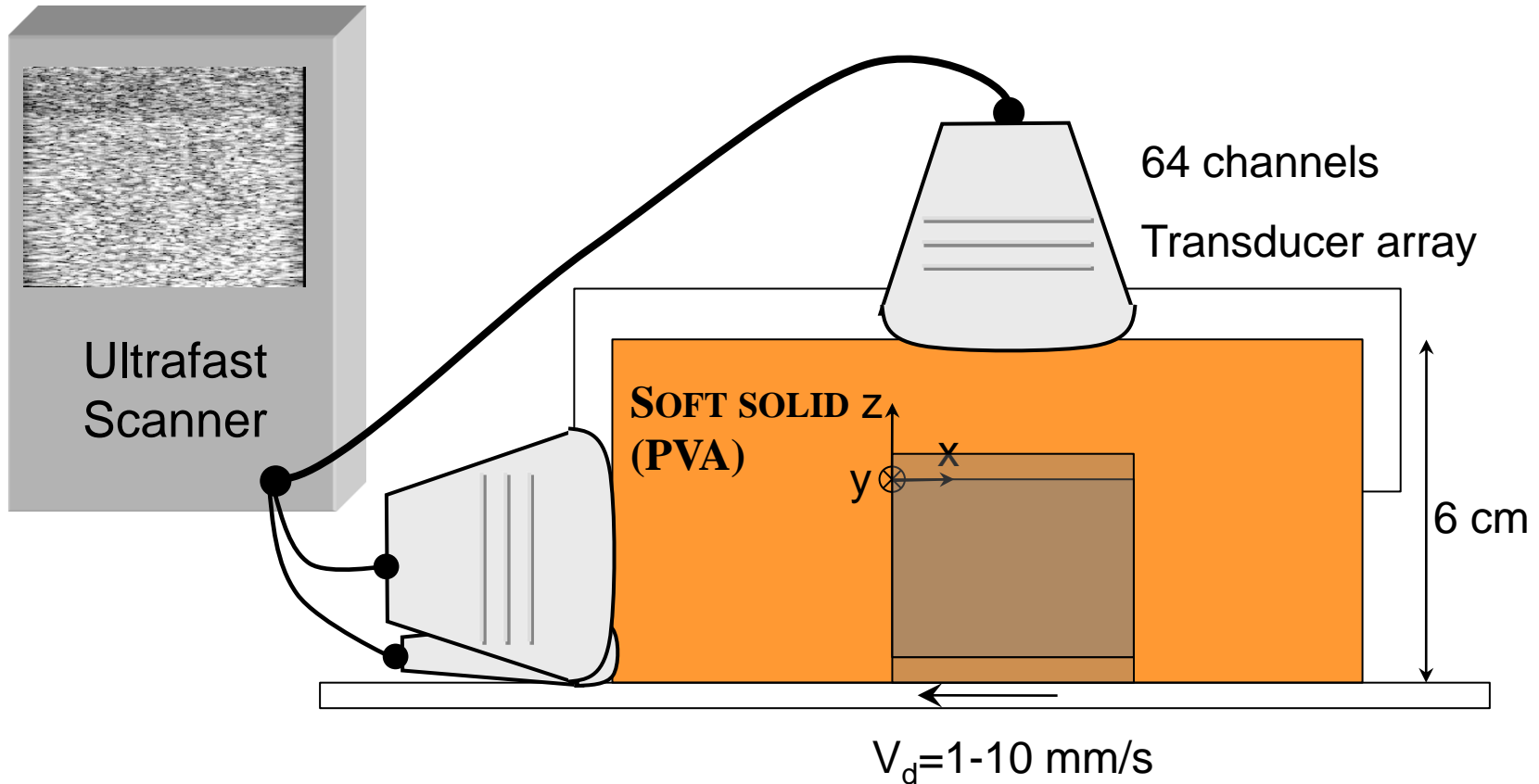
Stefan CATHELIN
Soumaya LATOUR
Thomas GALLOT
Francois RENARD
Christophe VOISIN
Michel CAMPILLO
Eric LAROSE

Earth Institute (ISTerre),
University of Grenoble

S. Latour *et al*,

« Ultrafast ultrasonic imaging of dynamic sliding friction in soft solids: the slow slip and the super shear regimes »
Europhysics Letter, EPL, 96 (2011) 59003.

Friction experimental set-up: the basic principle

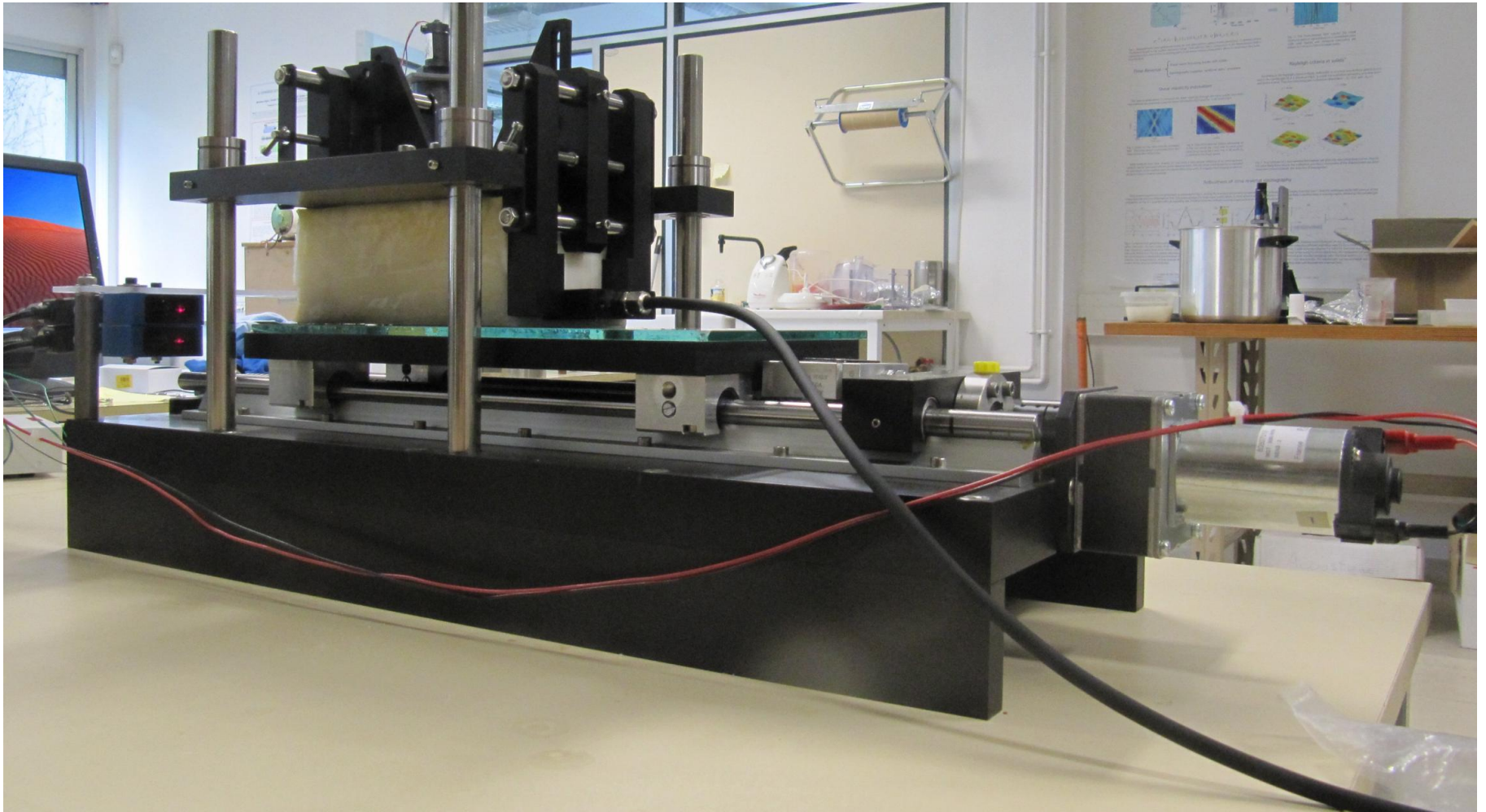


Soft: $V_S \sim 4$ m/s, $V_P \sim 1500$ m/s

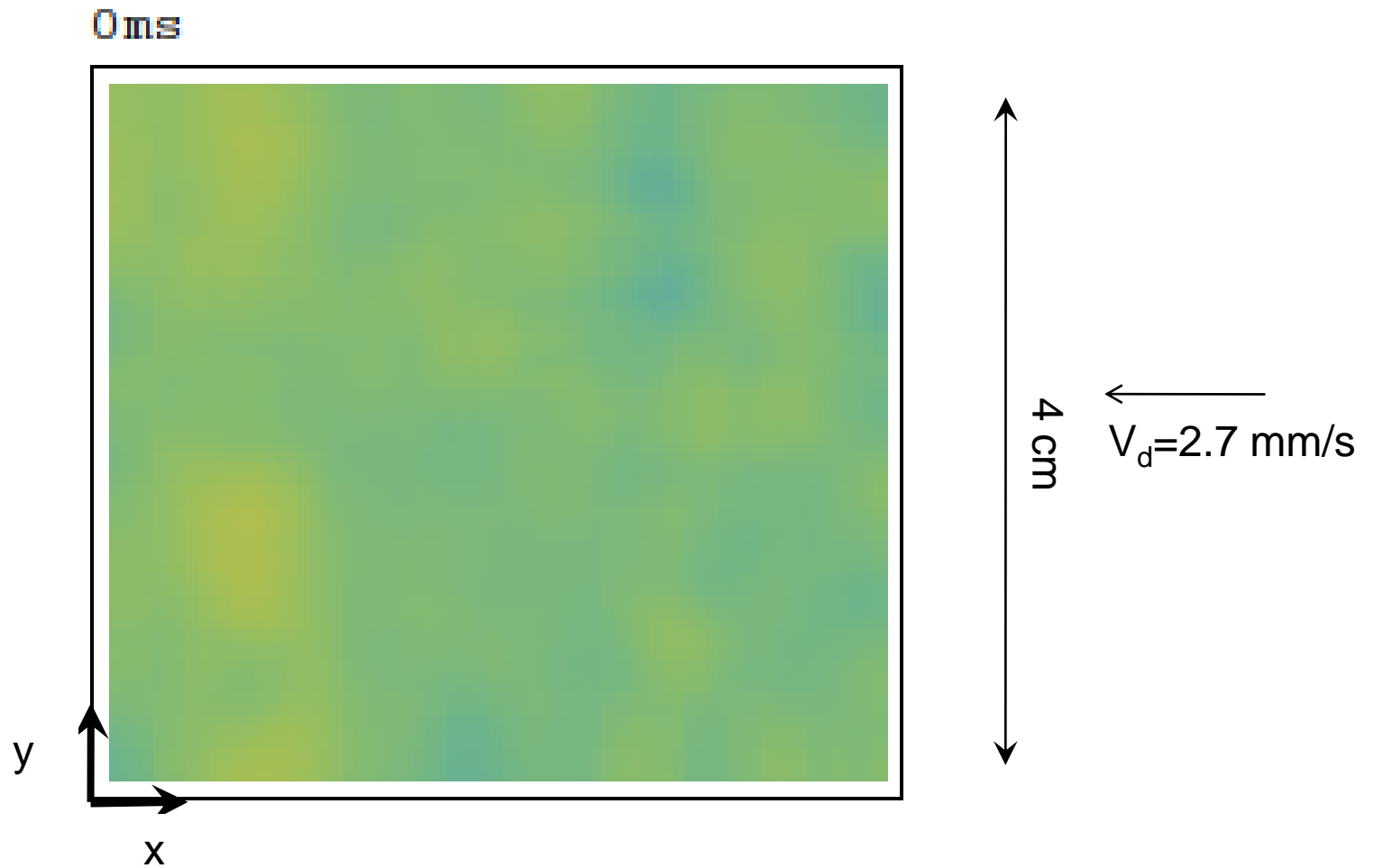
L. Sandrin, S. Catheline, M. Tanter, X Hennekin, M. Fink, « Time-resolved pulsed elastography with ultra fast imaging », *Ultrasonic Imaging* Vol. 13, pp.111-134, 1999.

Baumberger *et al.*, « Self-healing slip pulses and the friction of gelatin gels », *The European Physical Journal E*, Vol.11, pp.85, 2003.

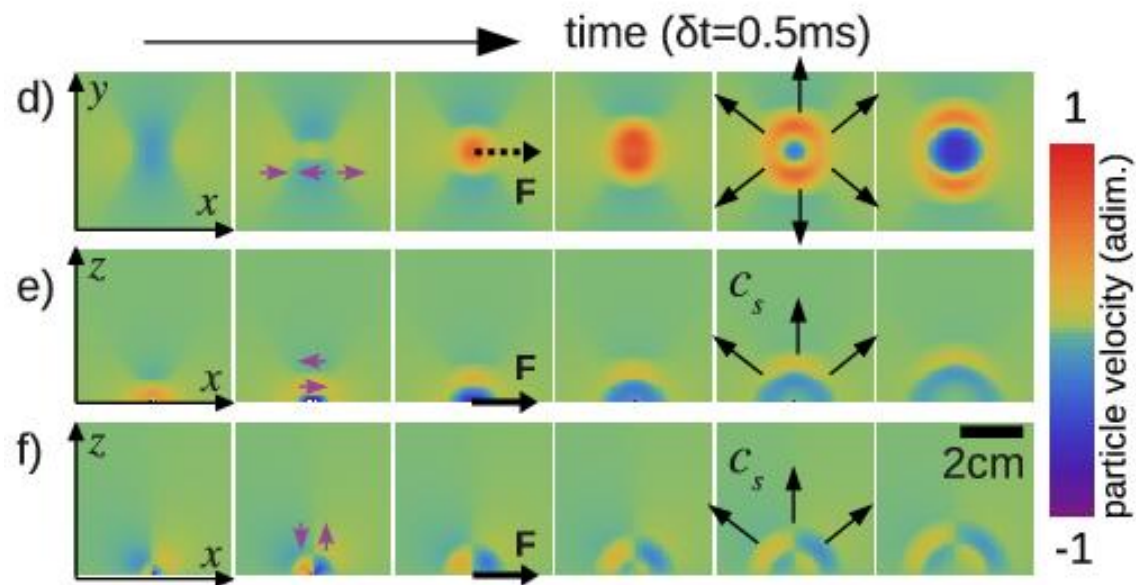
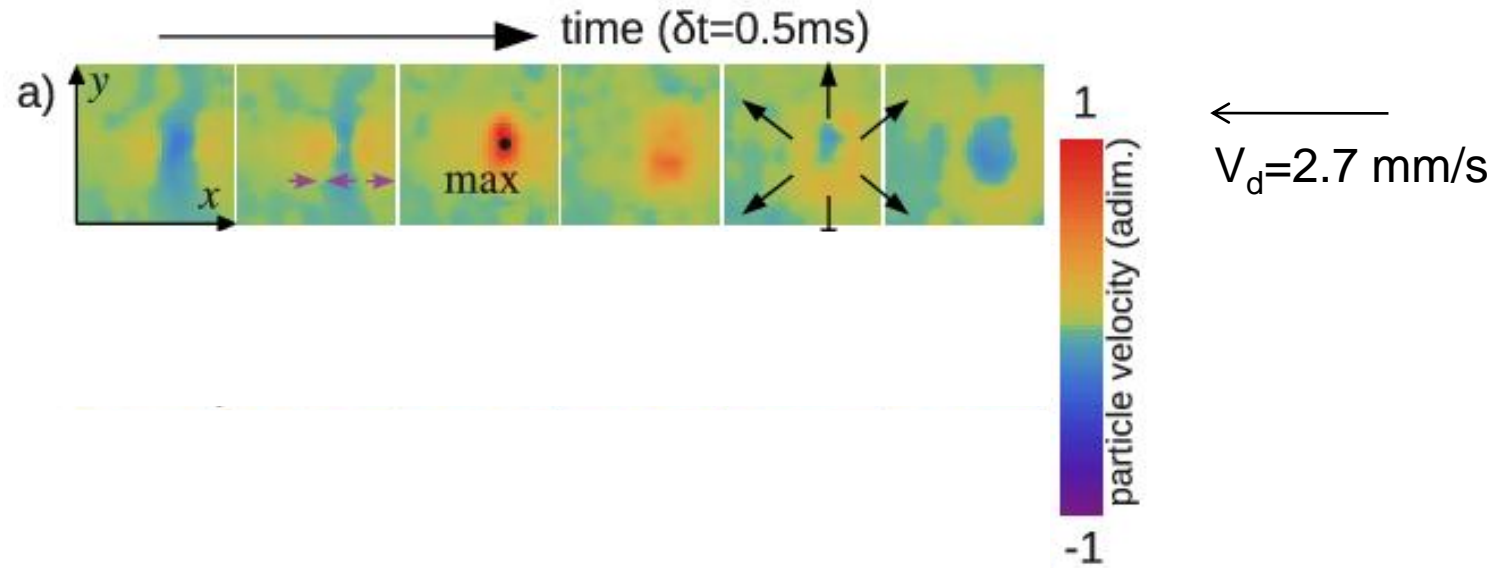
Experimental set-up



Strong friction configuration: PVA-sand paper interface



Strong friction configuration: Single depinning event analysis

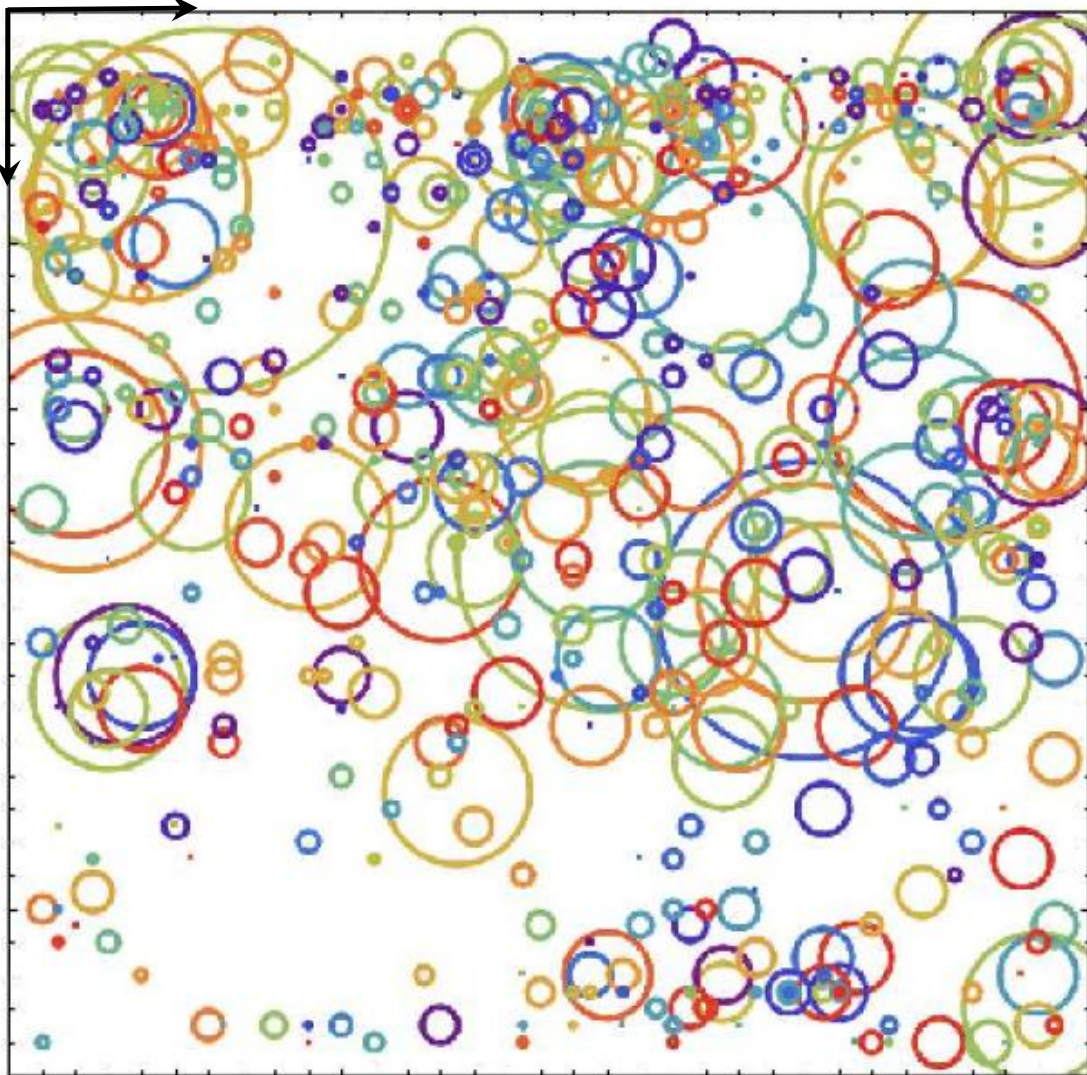


time (s)



y

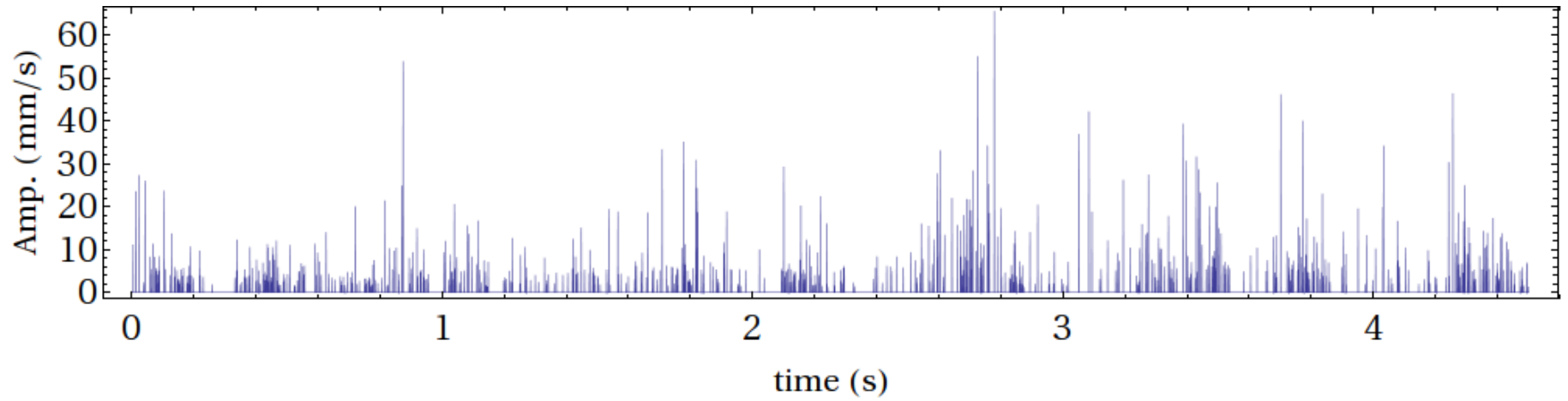
x



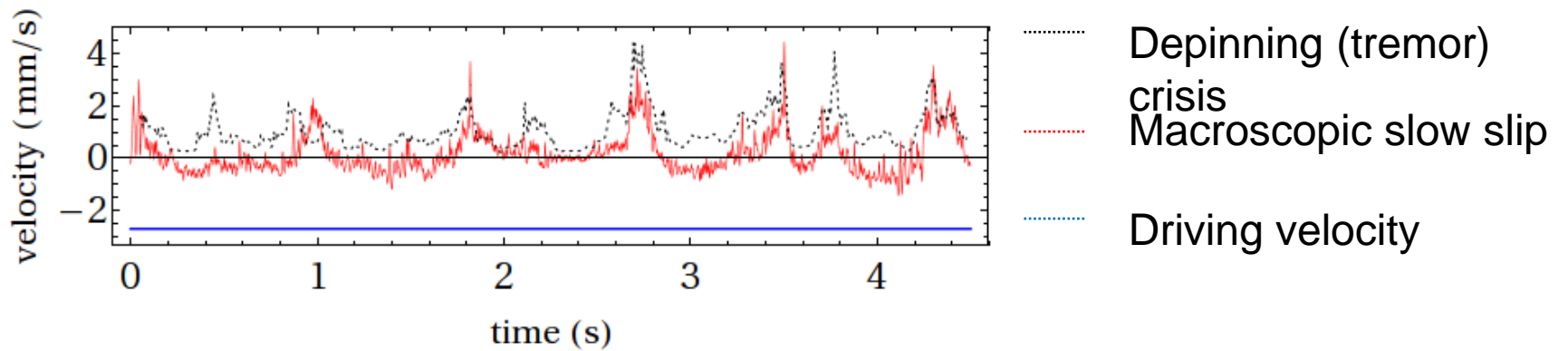
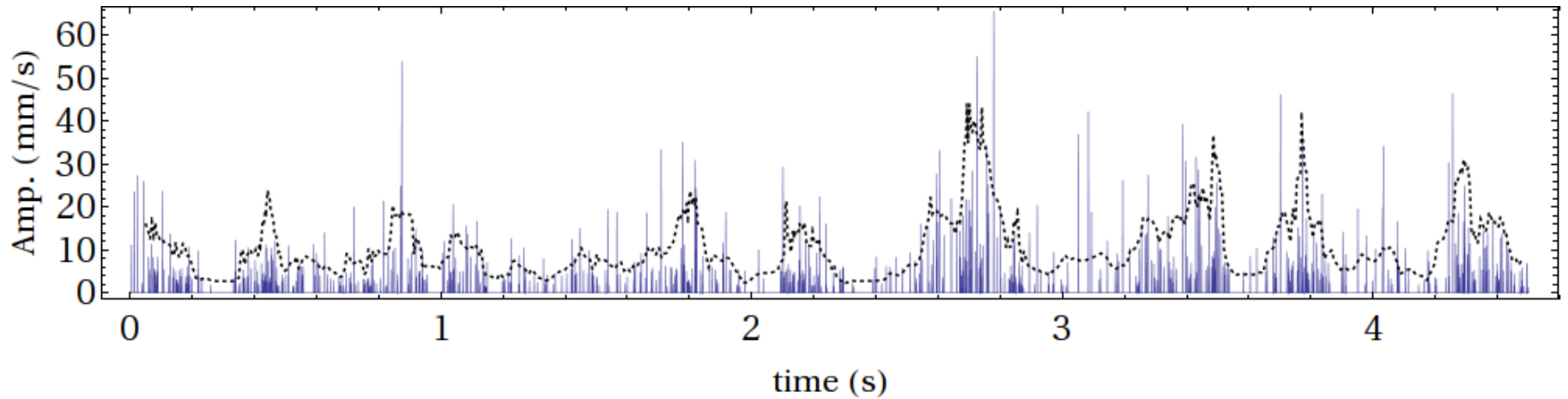
4 cm

$V_d = 2.7$ mm/s

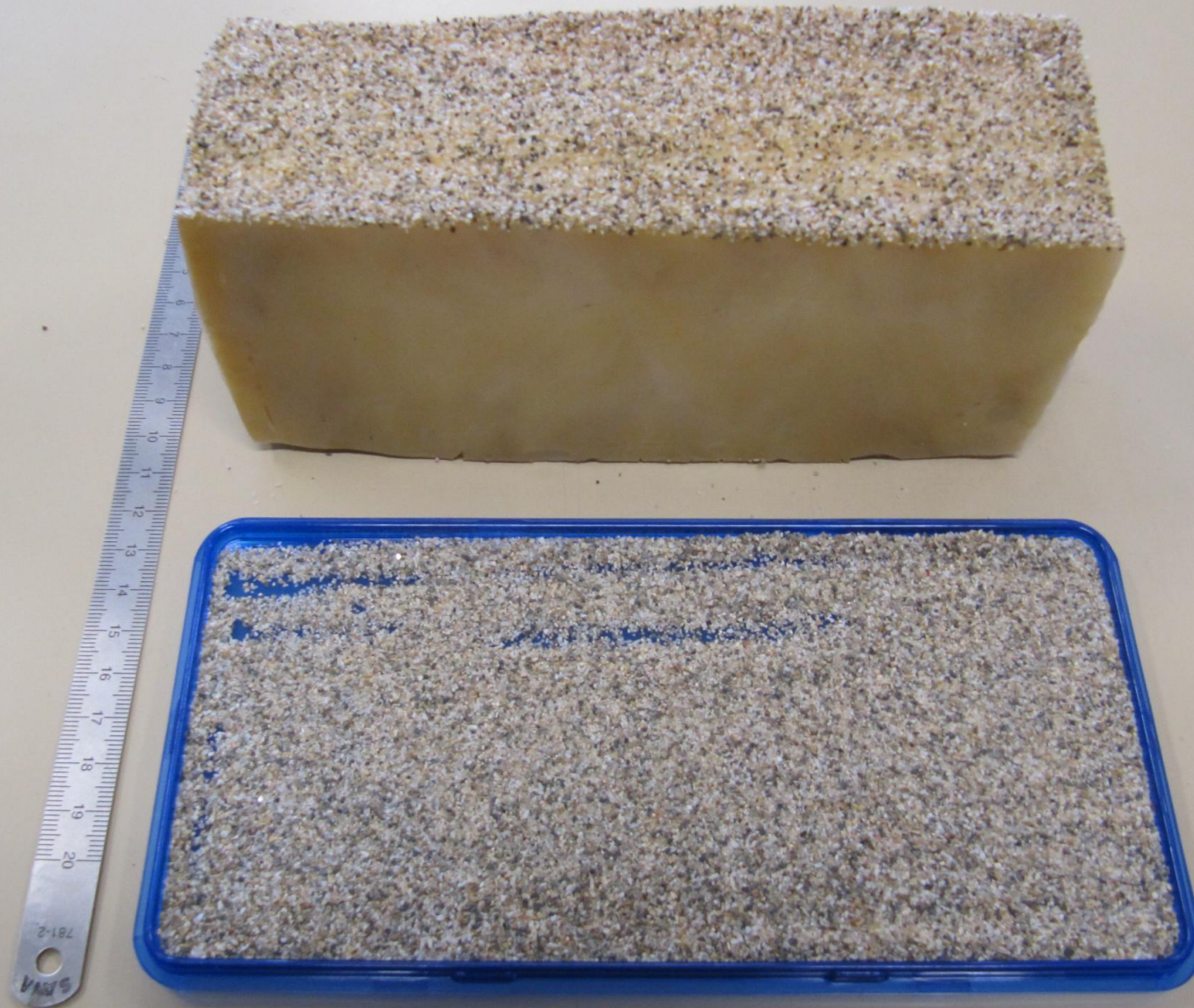
Strong friction configuration: Statistic analysis



Part I: PVA-sand paper interface - Statistic analysis



Weak friction configuration : Sand/glass interface



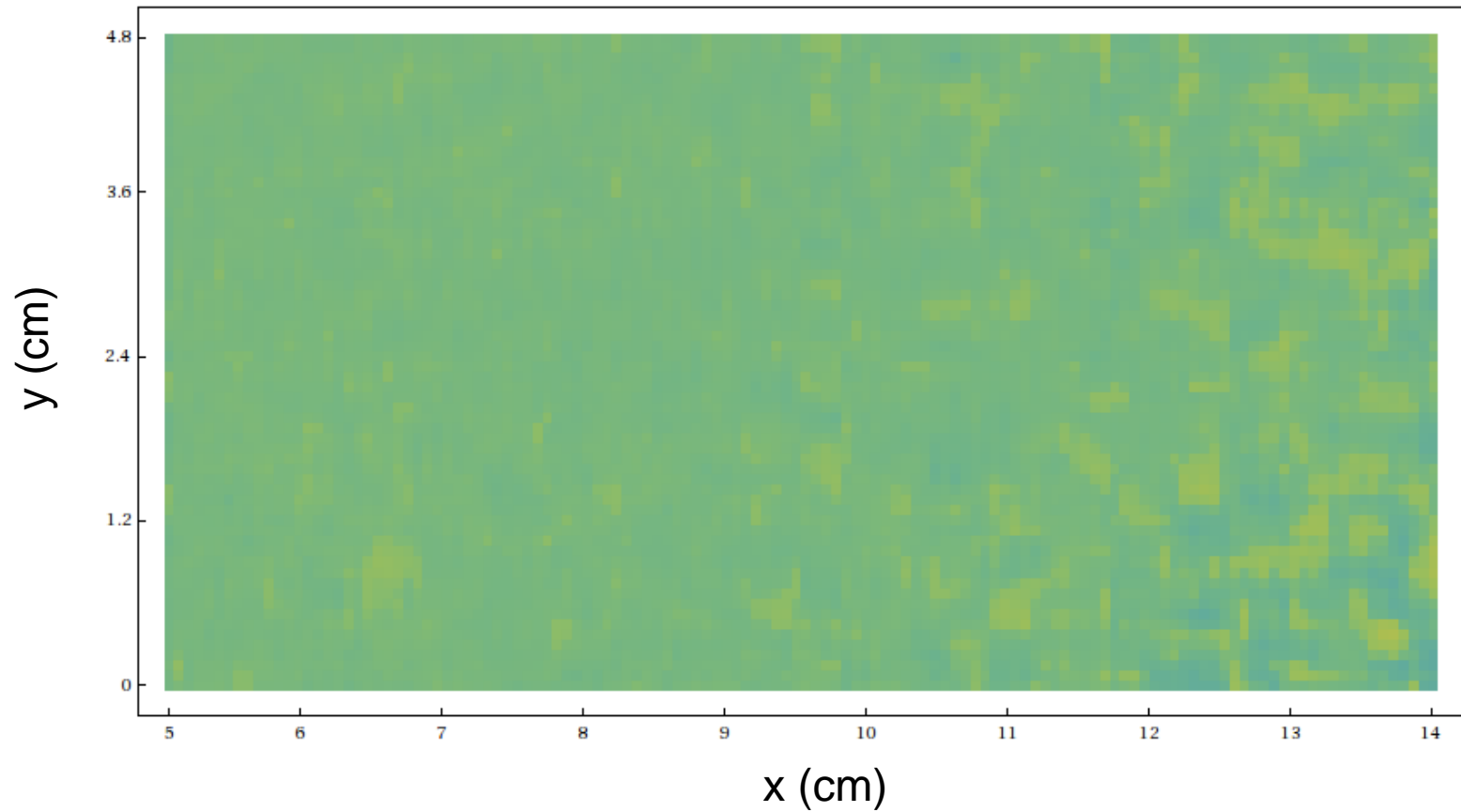
Weak friction configuration : Sand/glass interface



Weak friction configuration : super shear regime

Mach 2.5

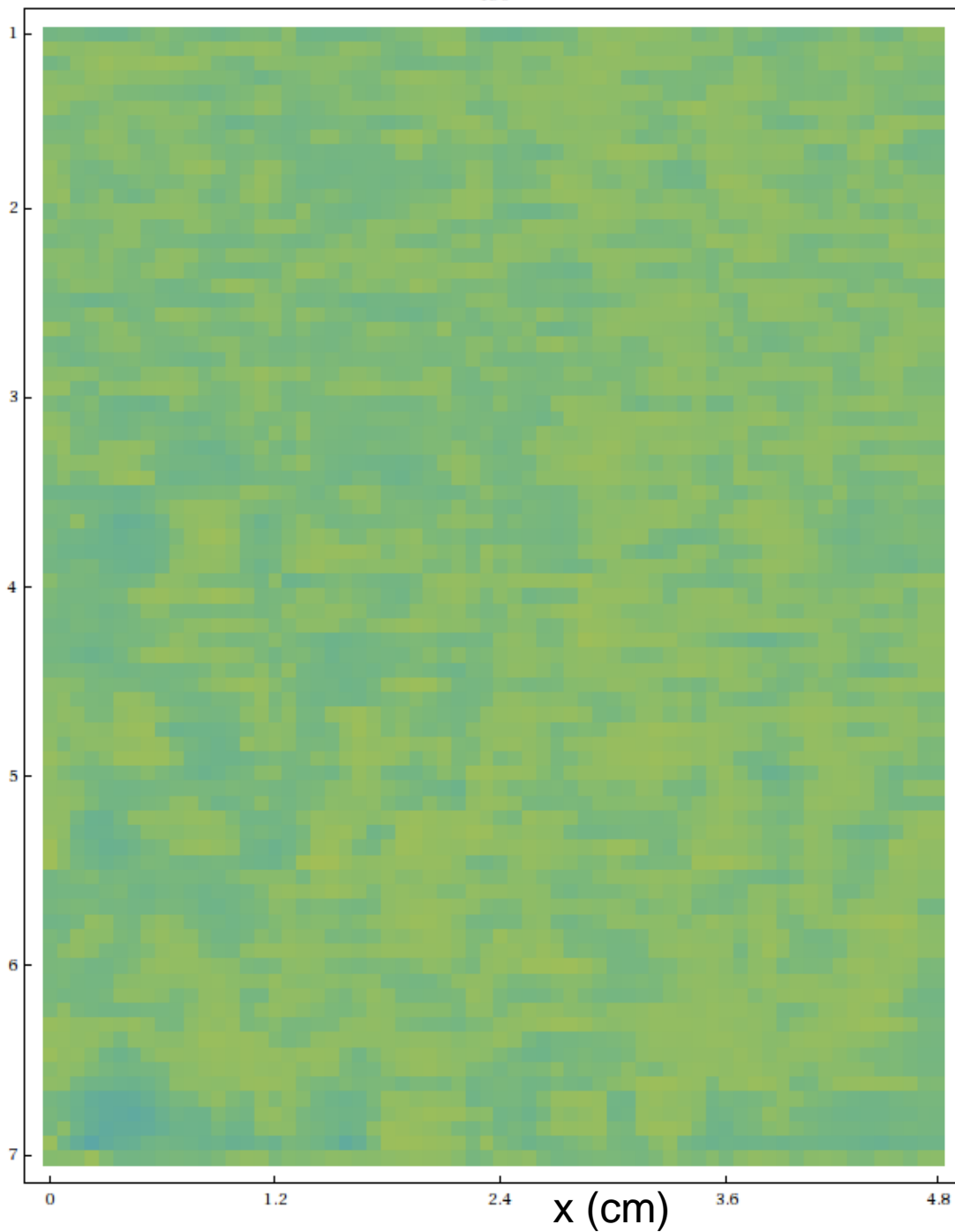
160



← $V_d = 1 \text{ mm/s}$

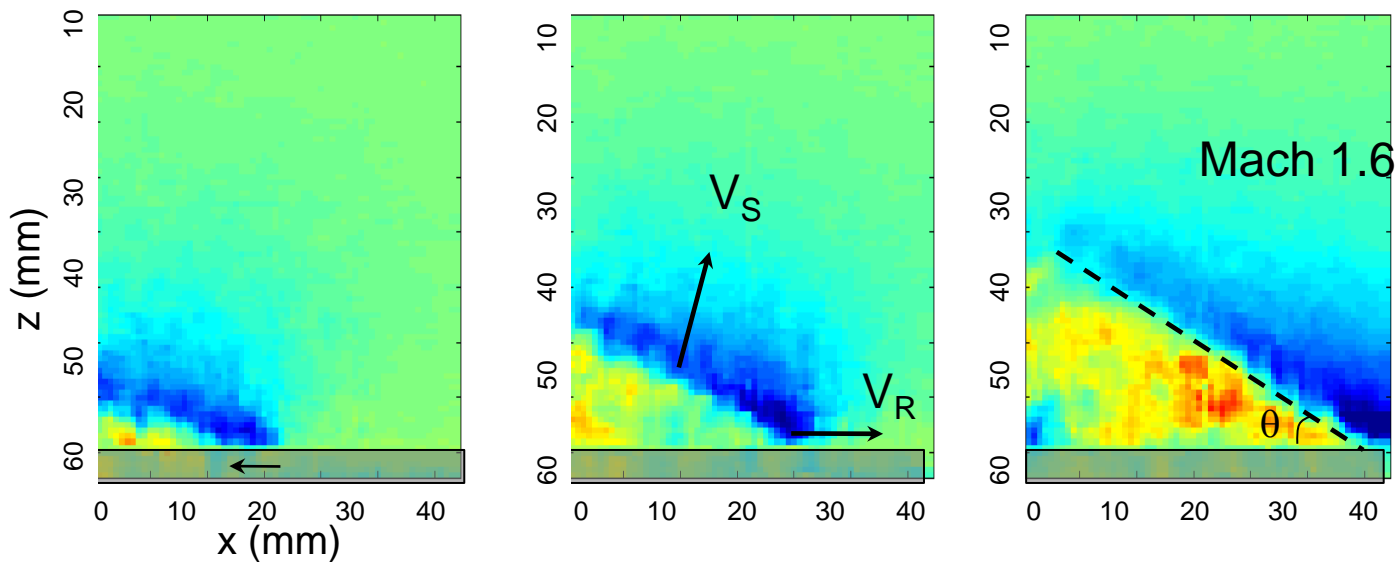
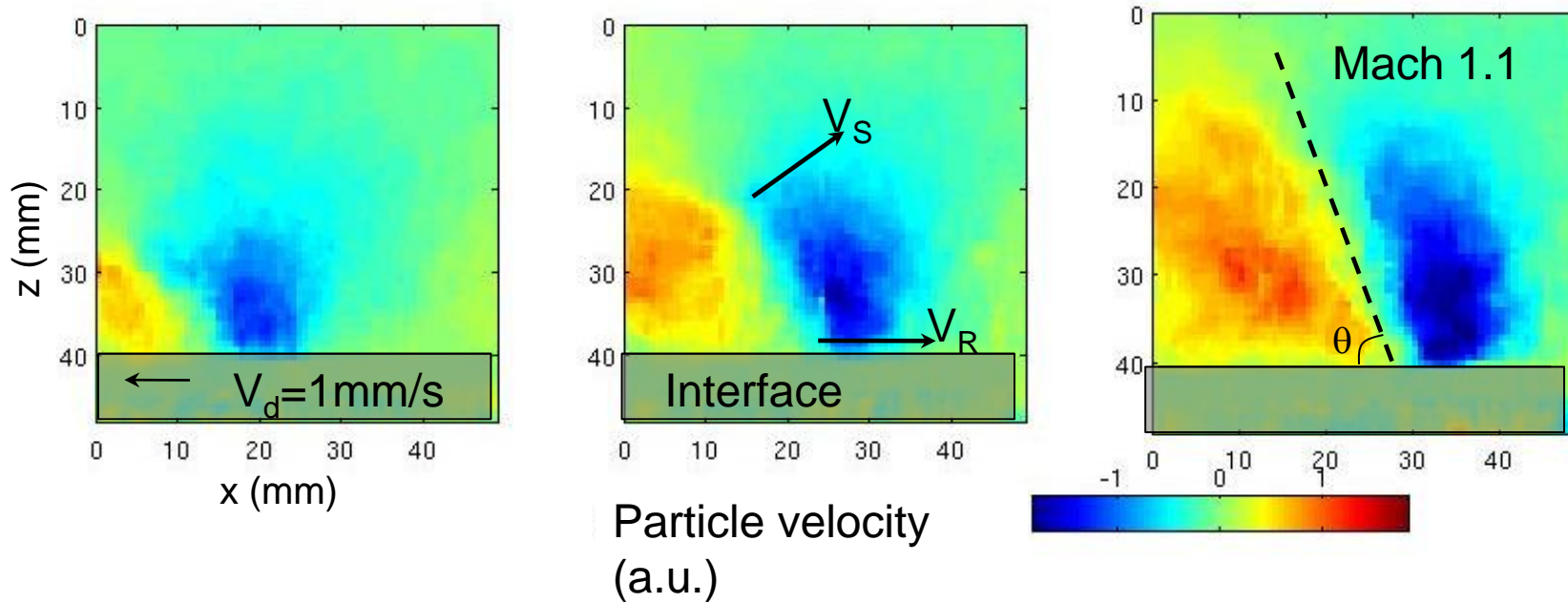
Mach 1.6

z (cm)

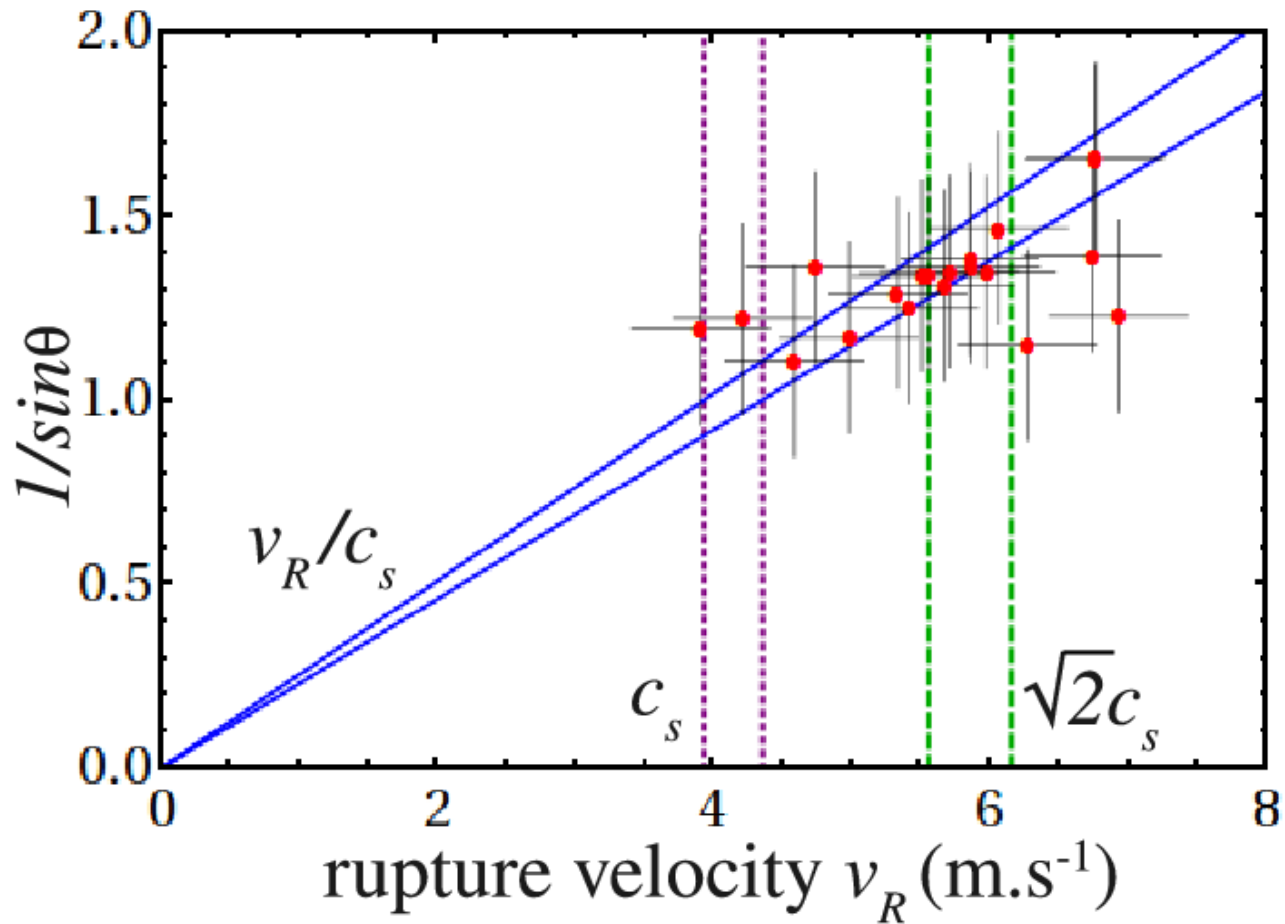


← $V_d = 1 \text{ mm/s}$

Weak friction configuration : super shear regime



Weak friction configuration : super shear regime



Mott (1945), Burridge (1973).

Archuleta R., Journal of Geophysical Research, Vol.89, pp.4559, 1984. 1979 Imperial Valley earthquake

A. Rosakis *et al.*, « Cracks faster than the shear wave speed », Science, Vol.284, pp.1337, 1999.

Effect of heterogeneities

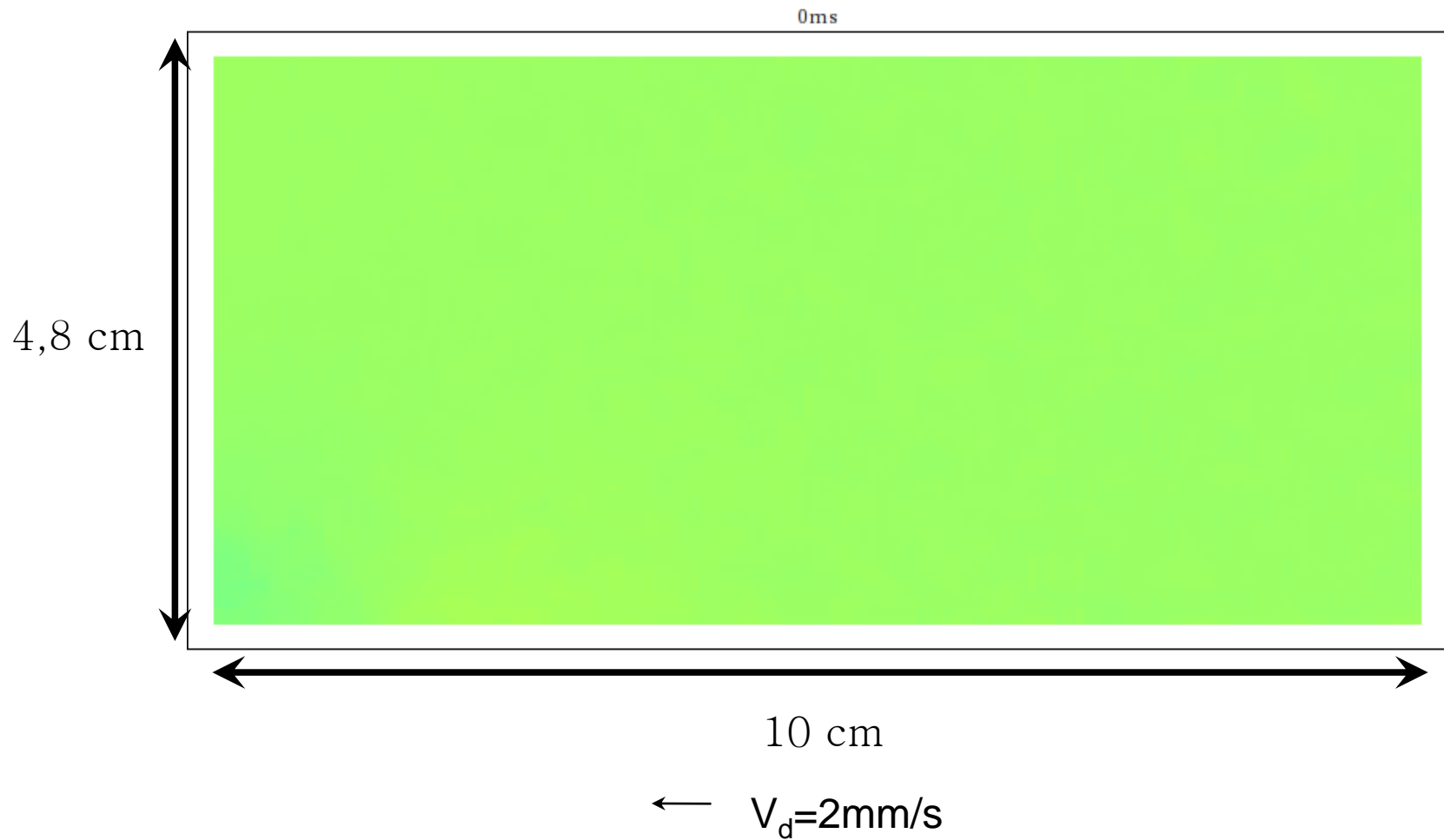
Mixed friction configuration: Sand+Pebbles(higher cohesive resistance)



O. Ben David *et al.*, « The dynamics of the onset of frictional slip », *Science*, Vol.330, pp.211, 2010.

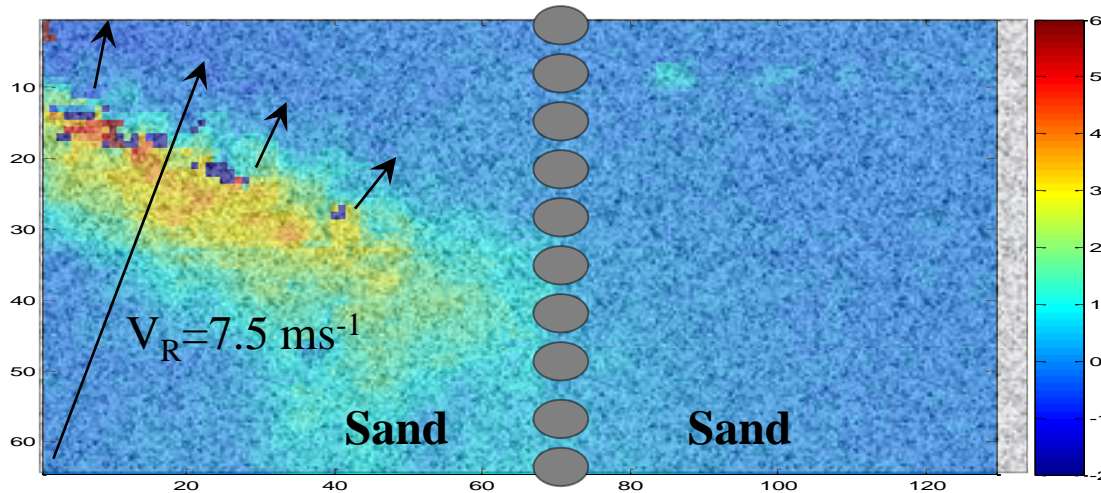
E. M. Dunham *et al.*, « A supershear transition mechanism for cracks », *Science*, Vol.299, pp.1557, 2003.

Effect of barriers



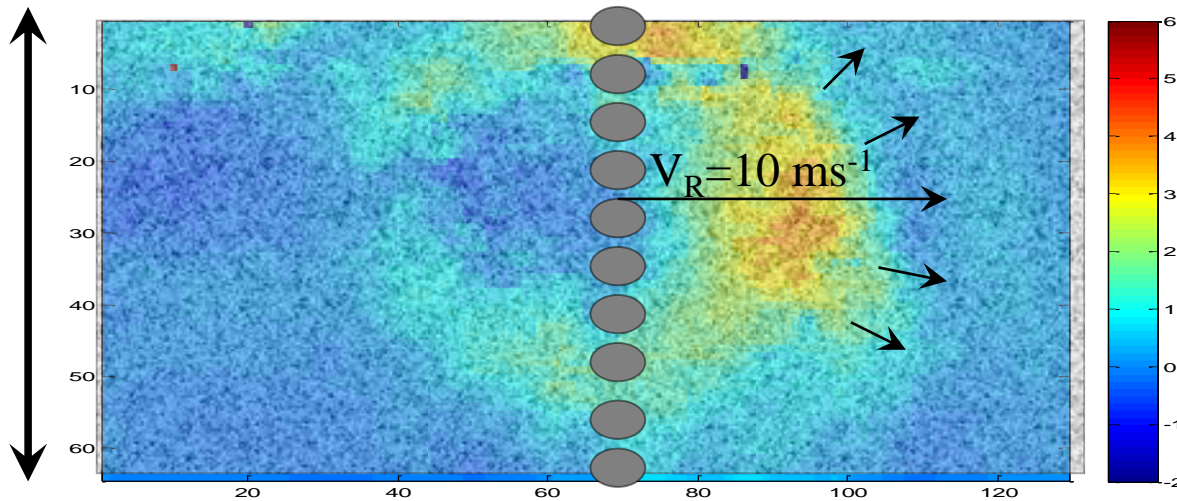
Mixed friction configuration

$V_S = 8 \text{ ms}^{-1}$
 $V_d = 2 \text{ mm.s}^{-1}$



Pebble barrier

4,8 cm



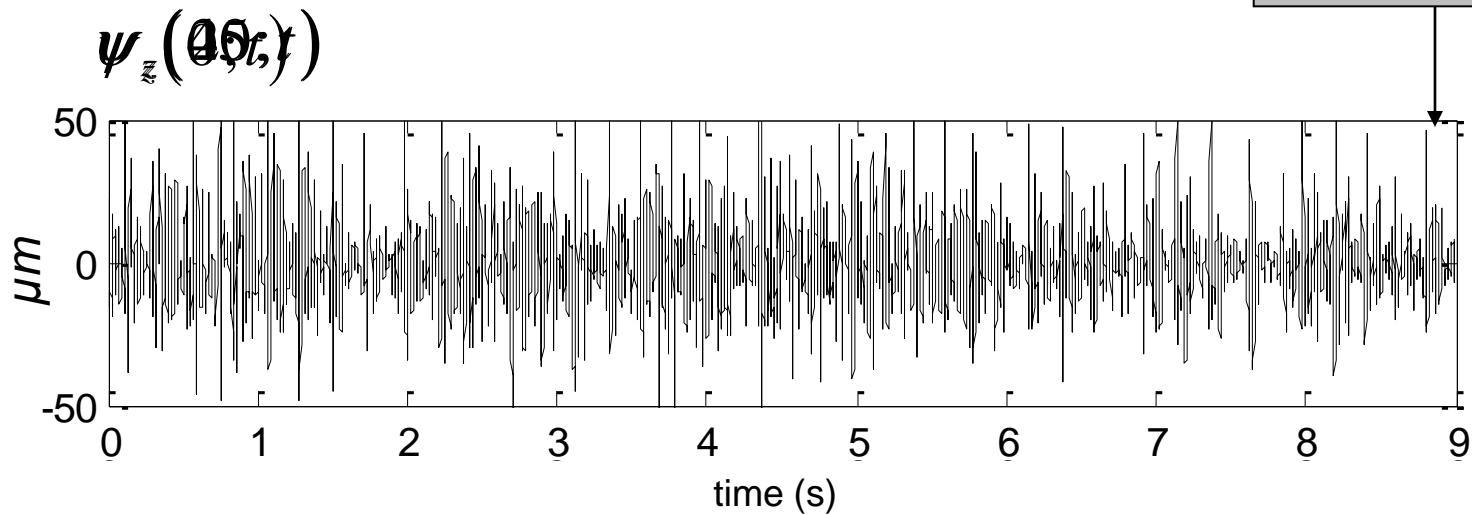
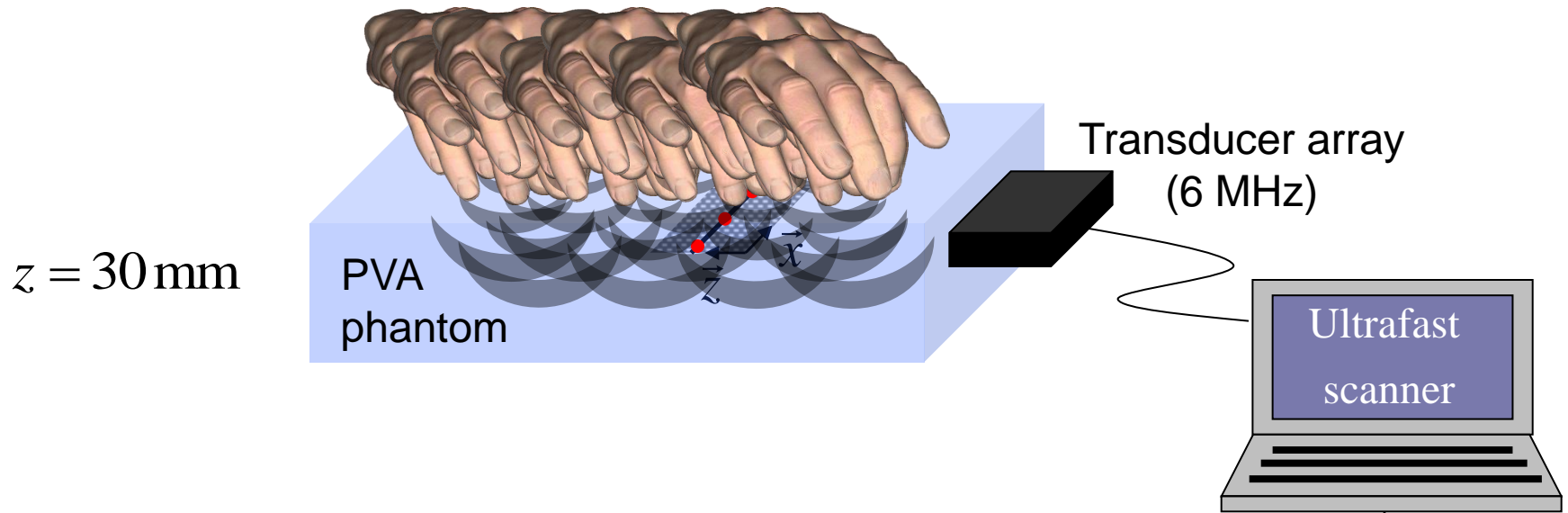
10 cm

Latour et al. « Effect of fault heterogeneity on rupture dynamics: an experimental approach using ultrafast ultrasound imaging », submitted Journal of Geophys. Research.

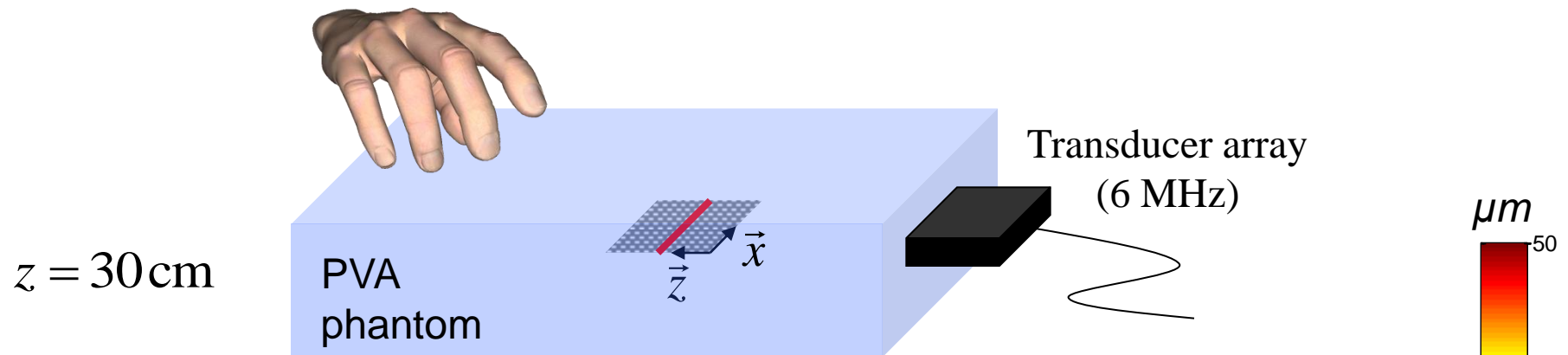
→ Non deterministic behaviour (memory effect?)

Part III: From seismology to medical imaging

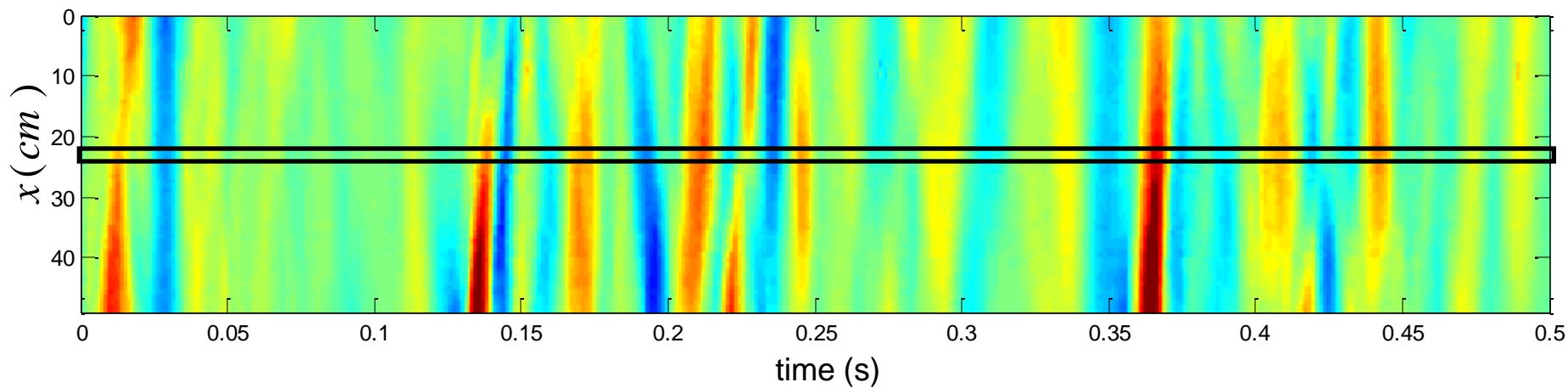
-Noise correlation technique in passive elastography-



Displacement field along the x -axis

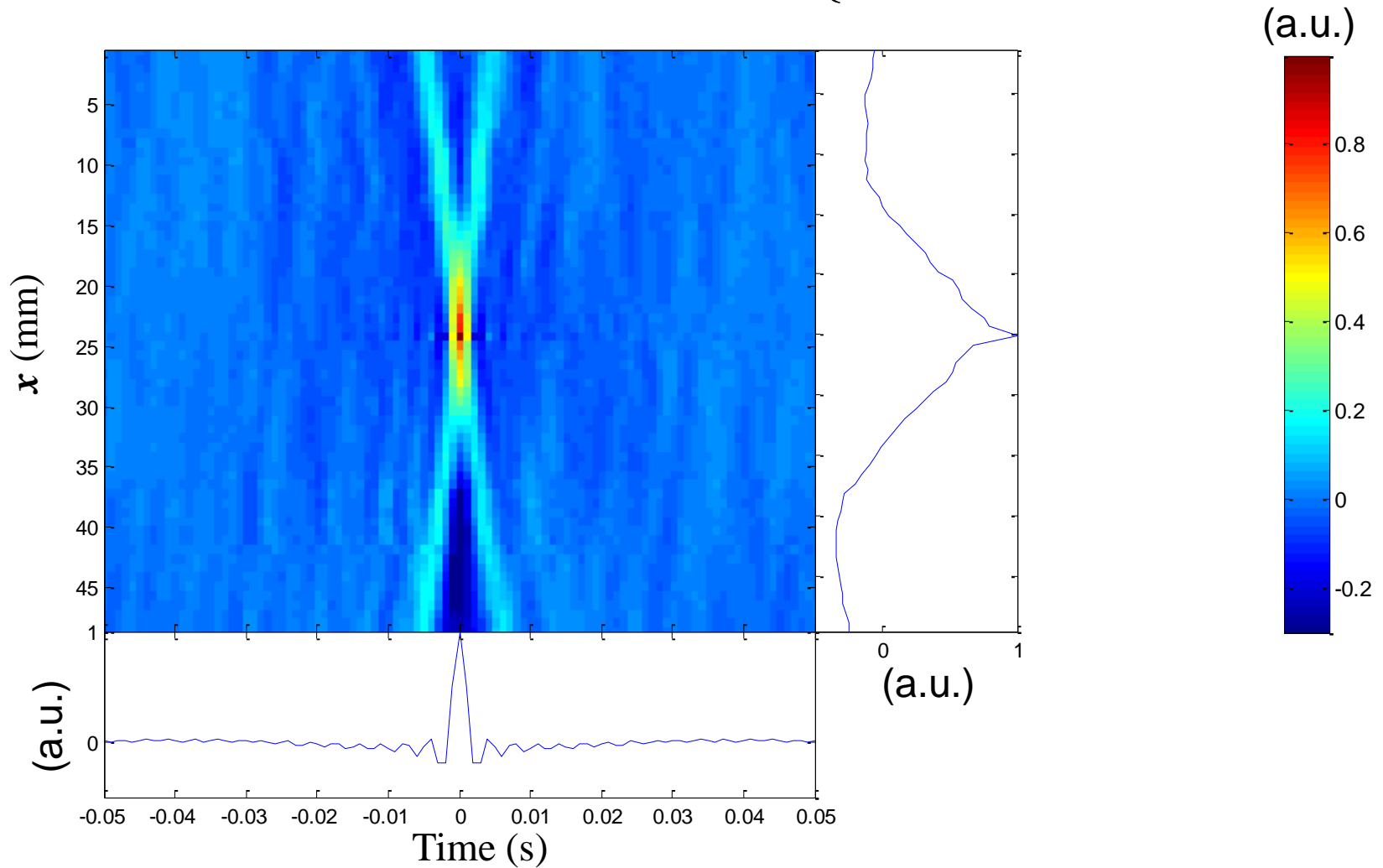


Zoom of half a second of $\psi_z(x;t)$ along x -axis

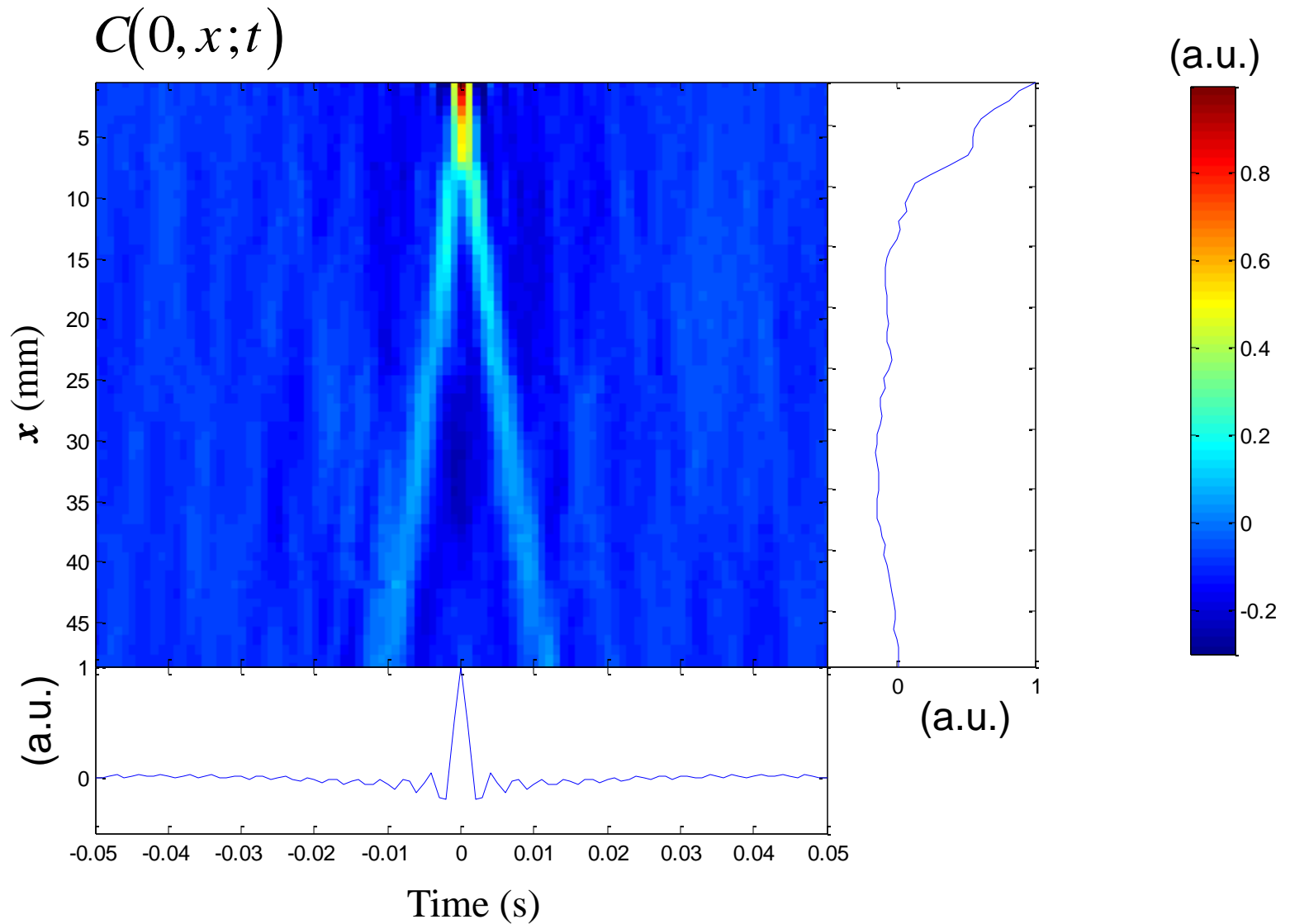


TR field from noise cross-correlation

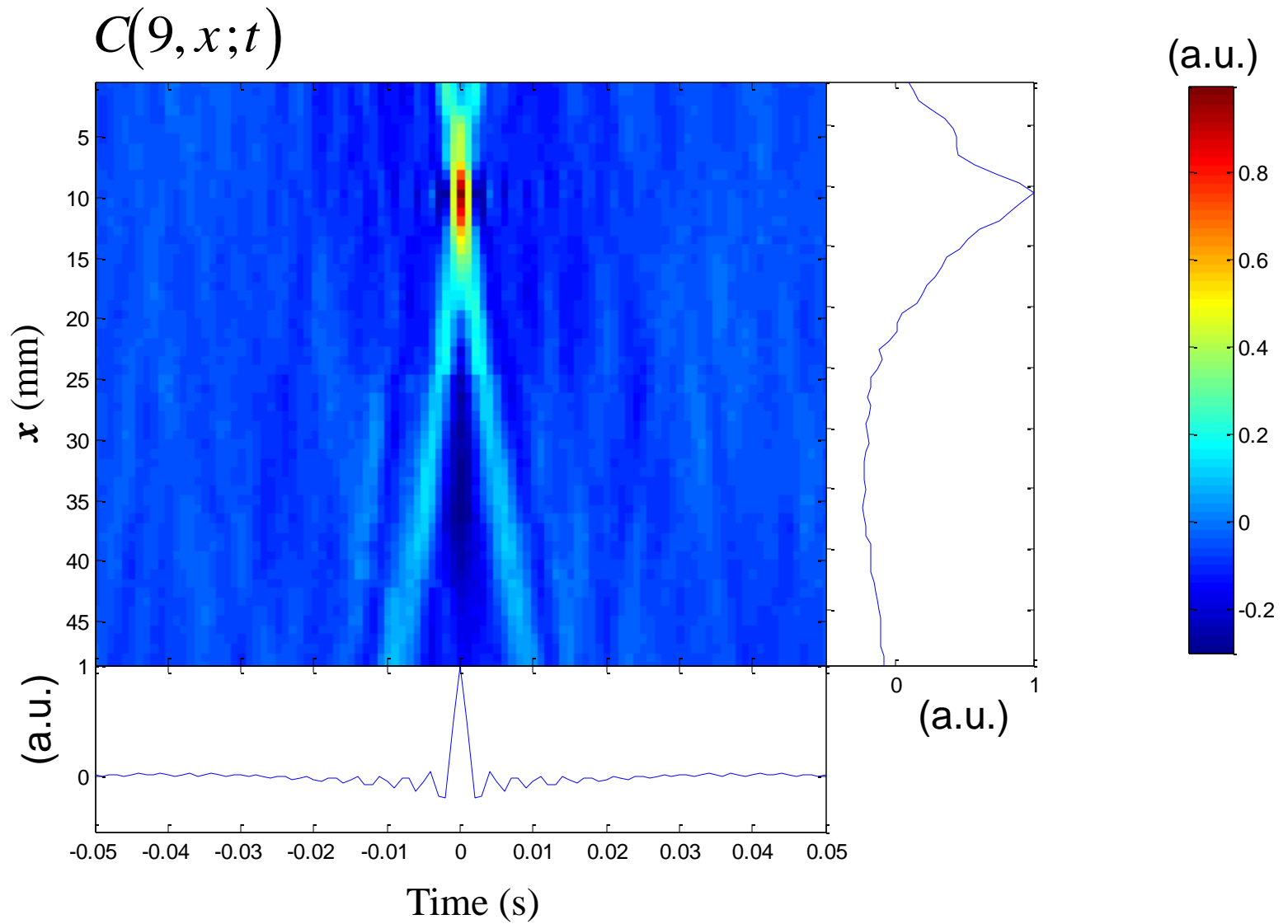
$$C(x_0, x; t) = \psi_z(x_0, T-t) \otimes \psi_z(x, t) \quad \begin{cases} x_0 = 24\text{mm} \\ x \in [0; 49] \end{cases}$$



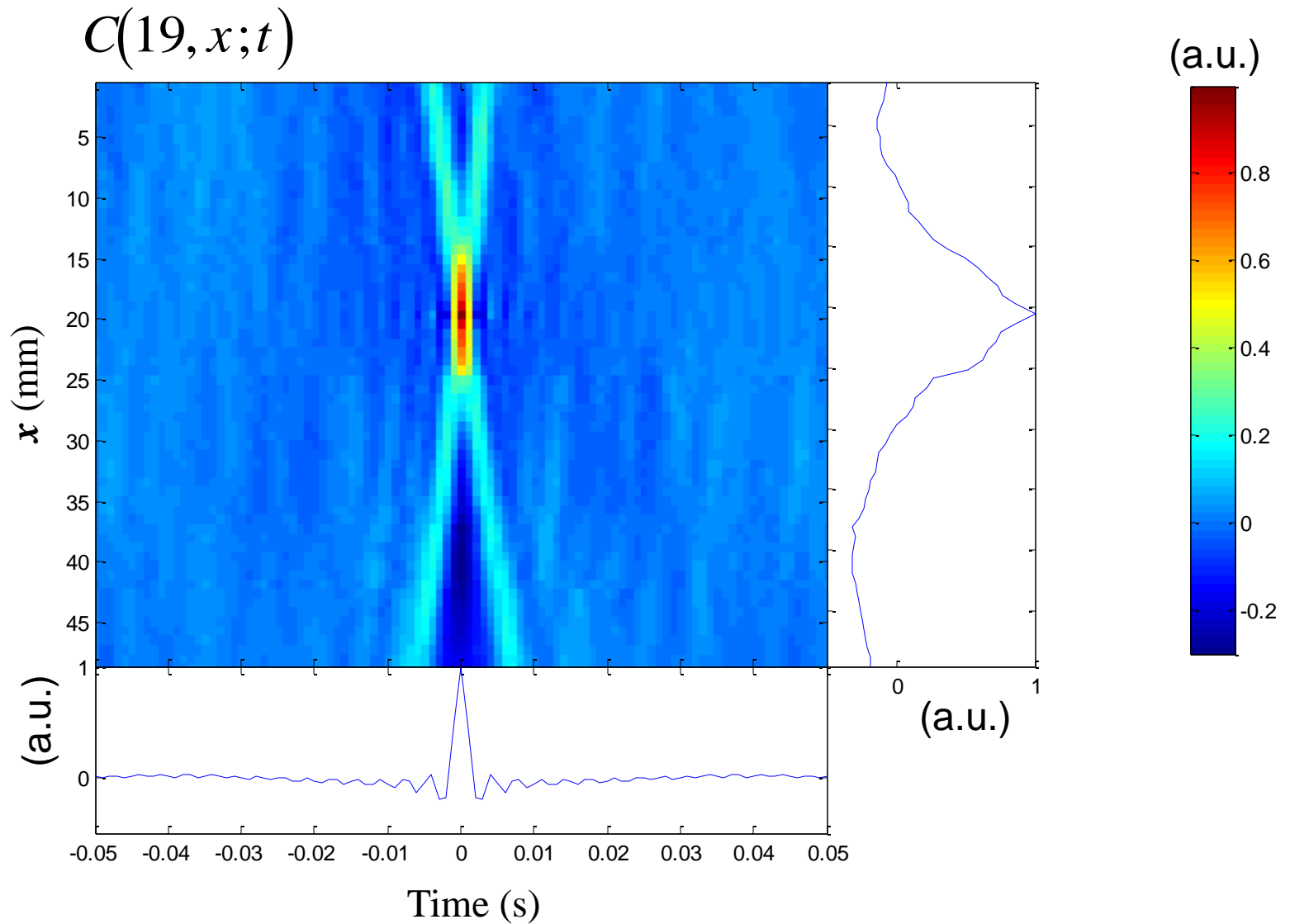
TR field from noise cross-correlation



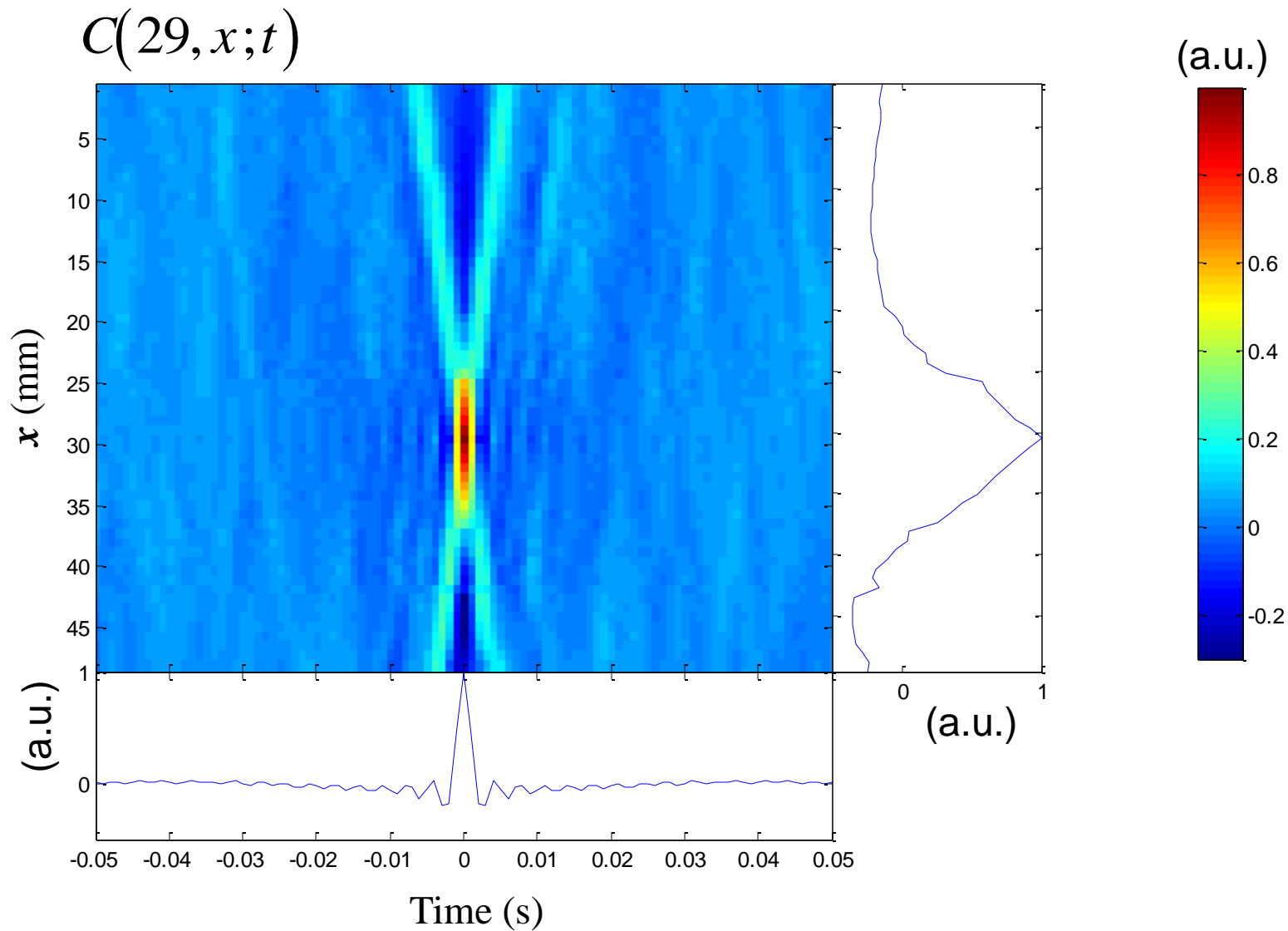
TR field from noise cross-correlation



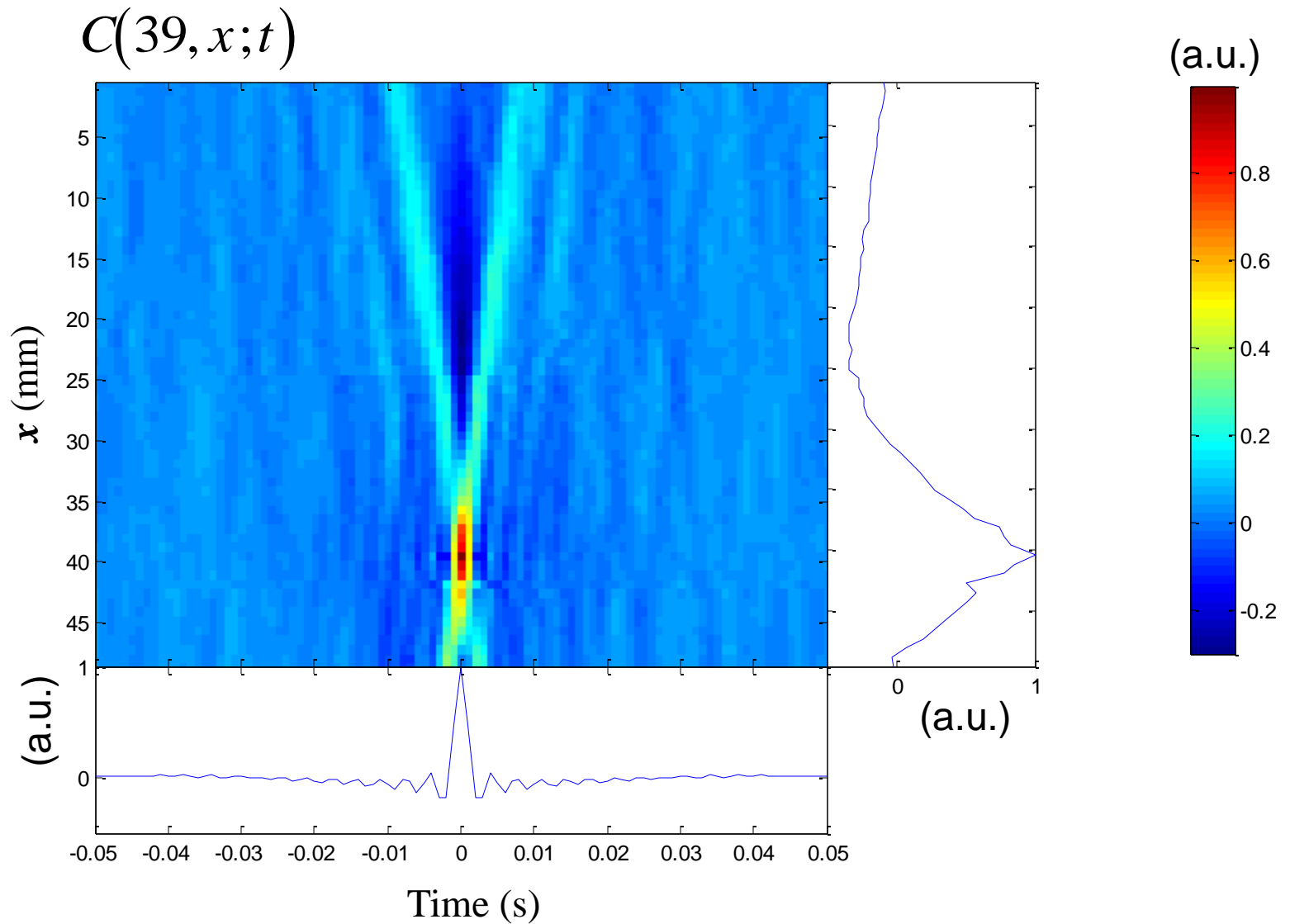
TR field from noise cross-correlation



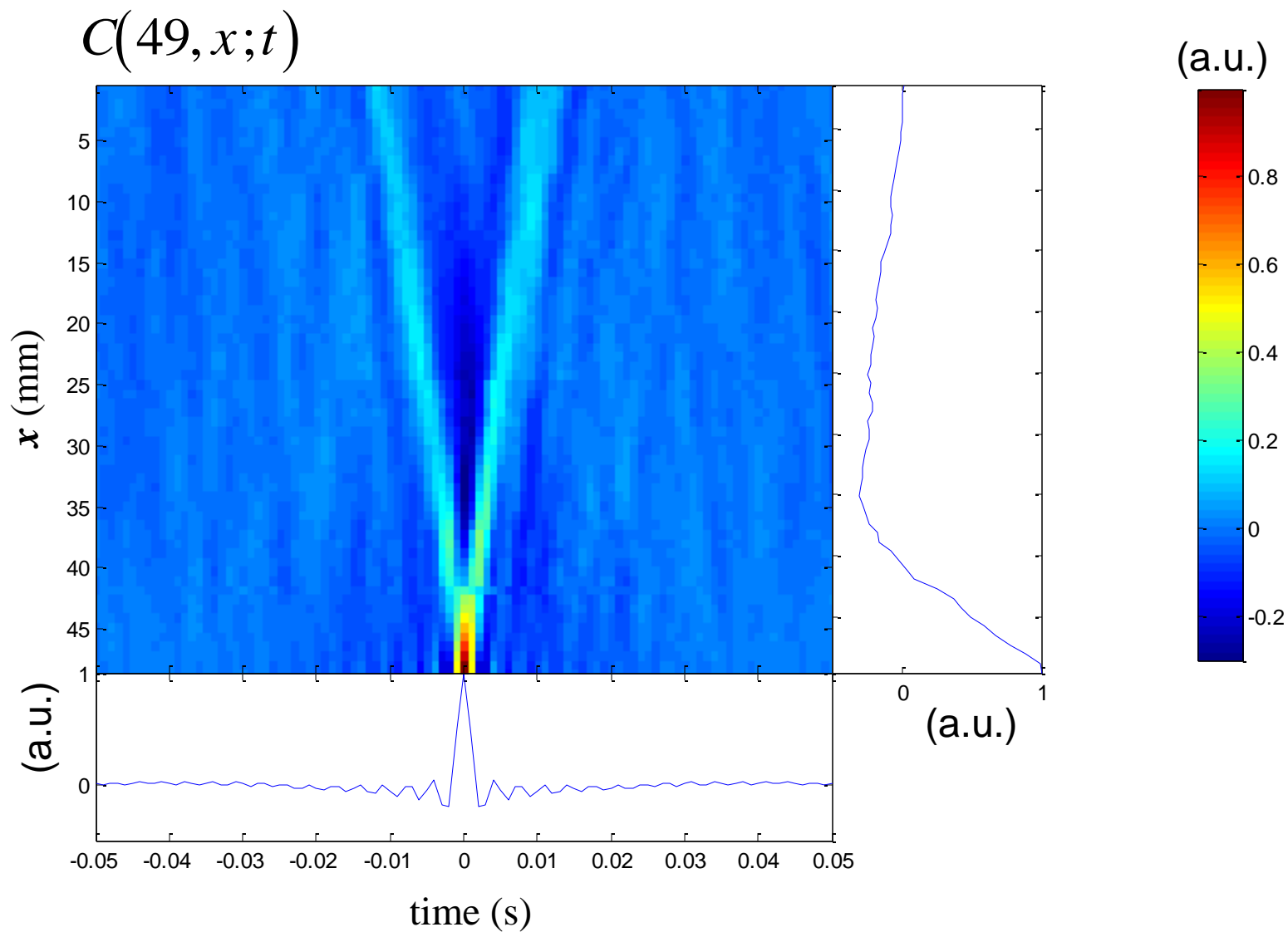
TR field from noise cross-correlation

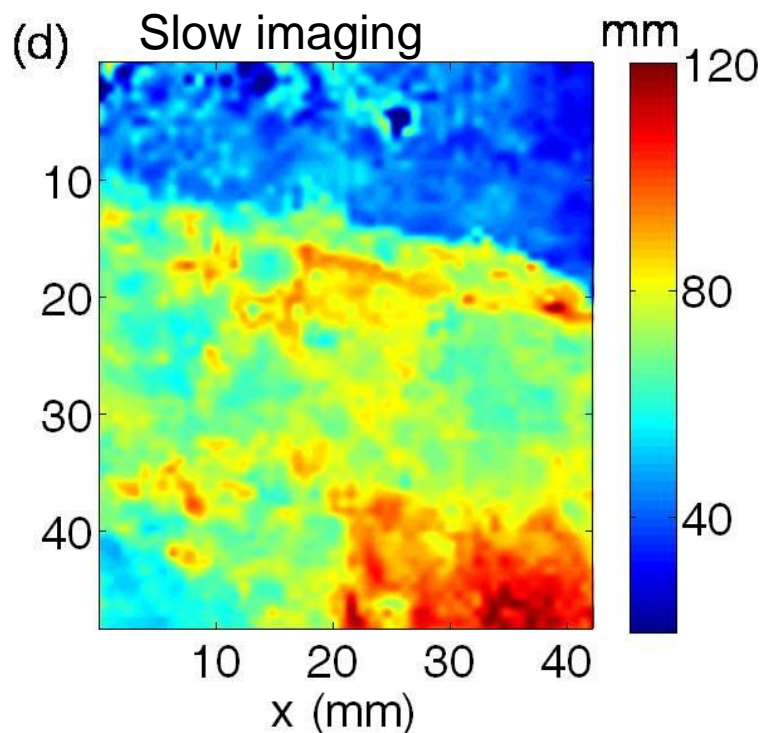
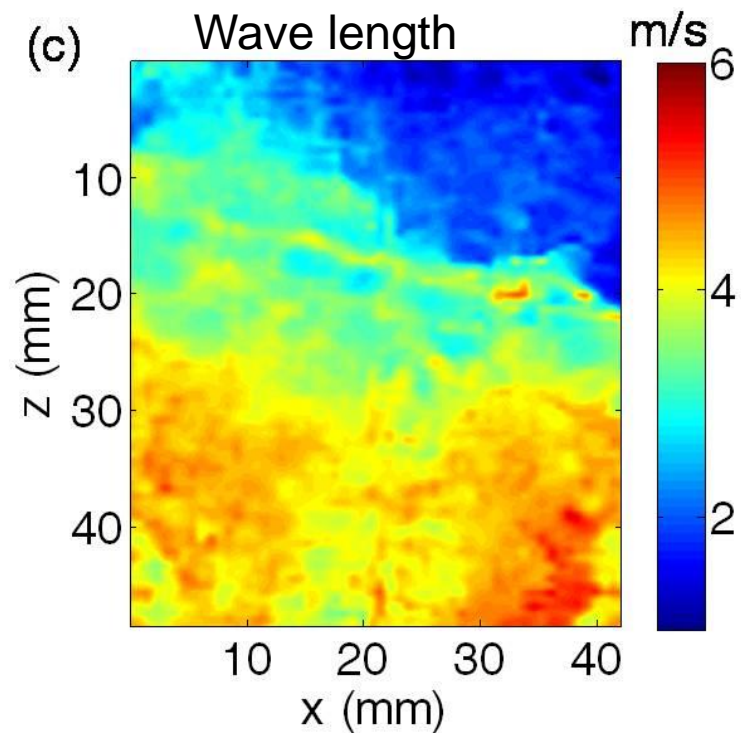
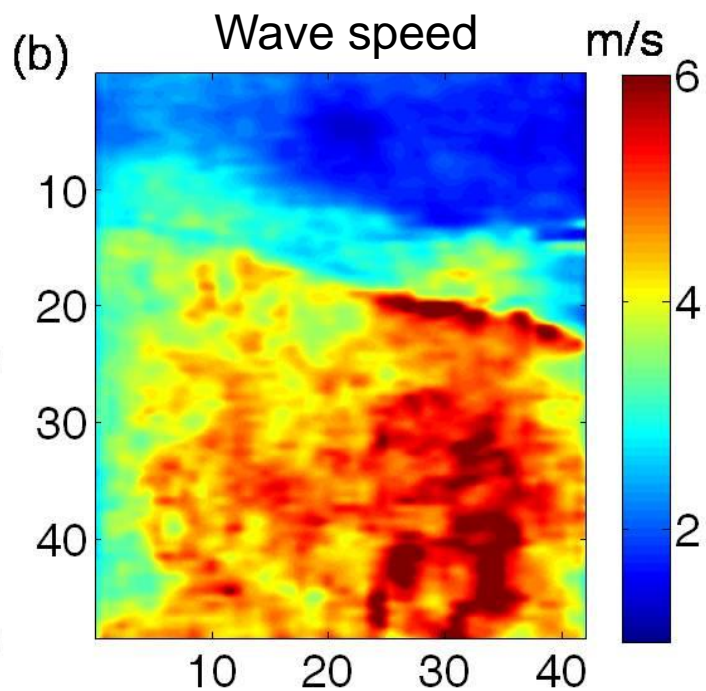
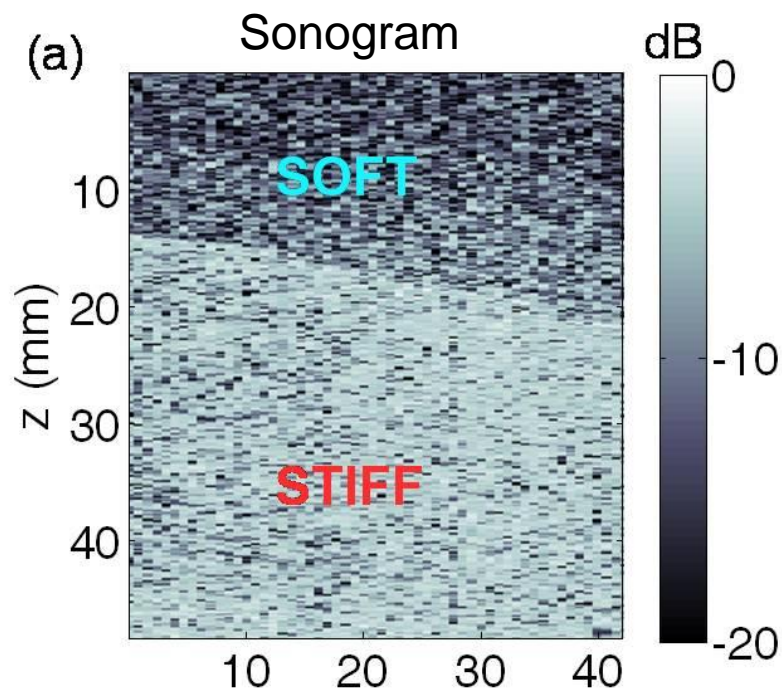


TR field from noise cross-correlation

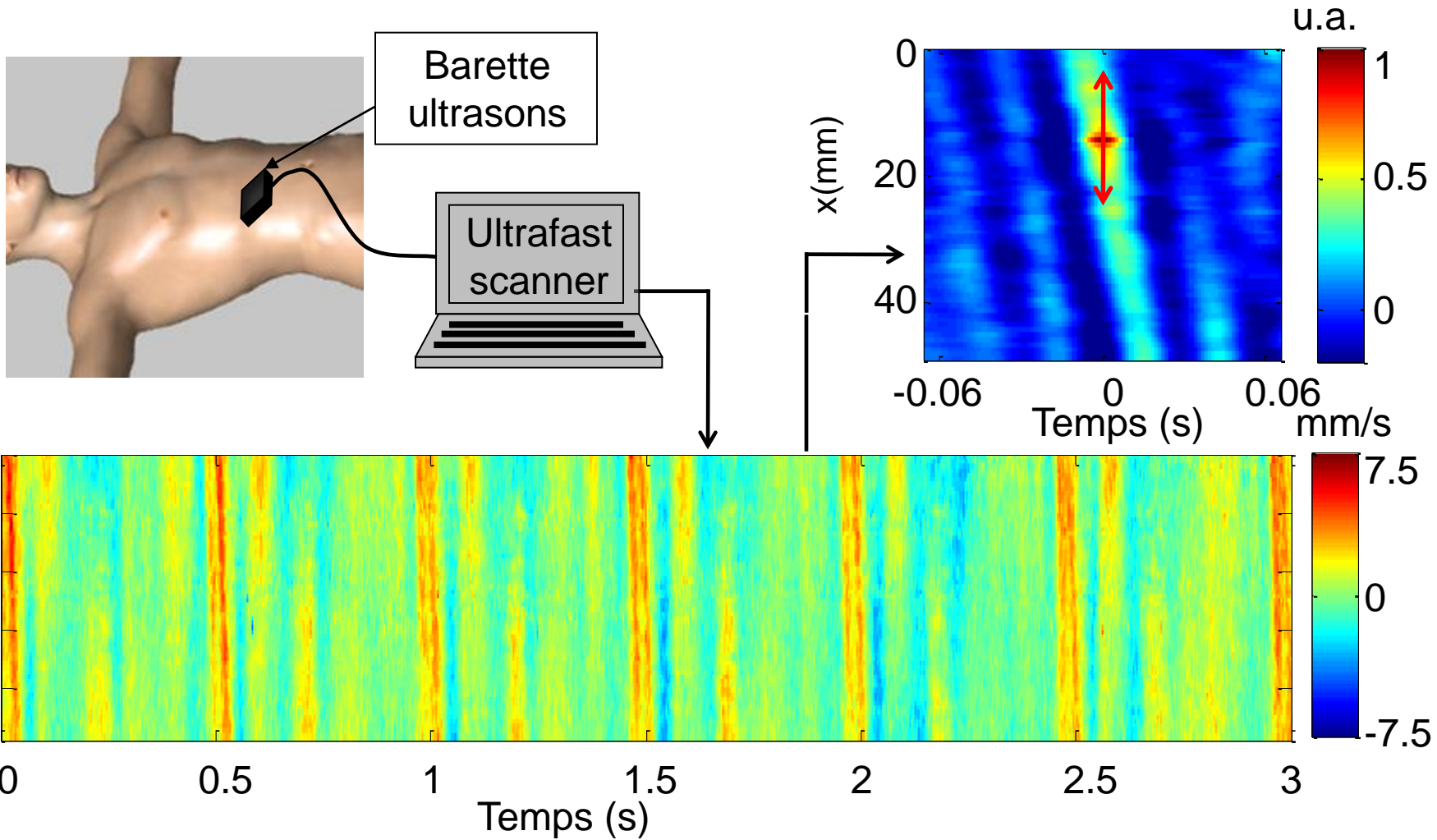


TR field from noise cross-correlation





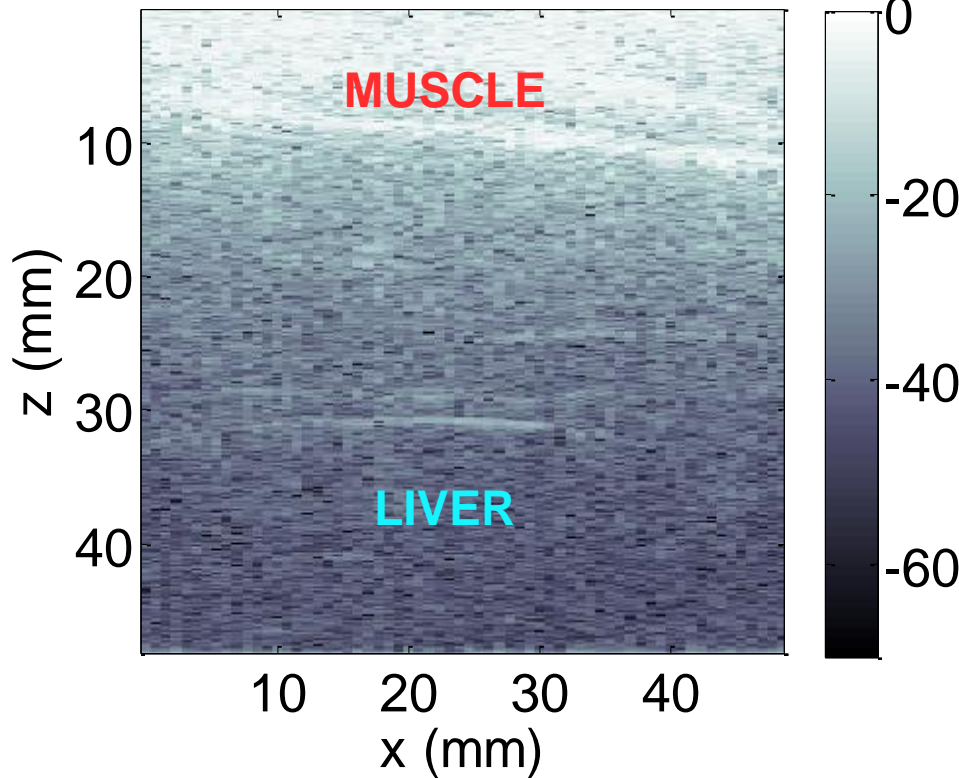
The physiologic noise correlation by use of elastography



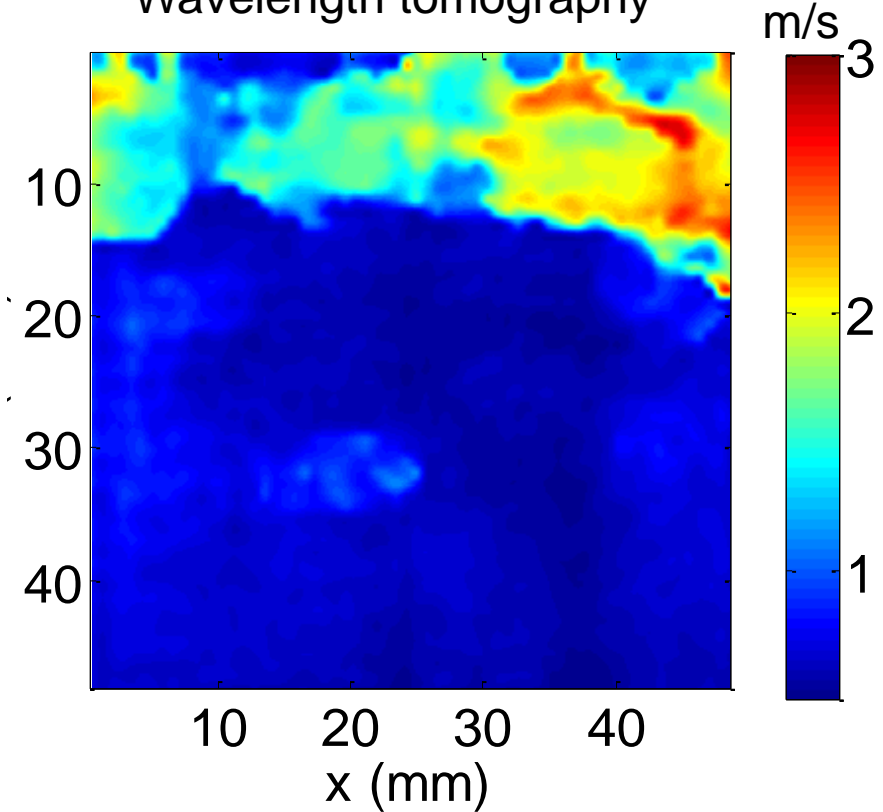
K. Sabra, S. Conti, P. Roux, and W. Kuperman, "Passive in vivo elastography from skeletal muscle noise," *Appl. Phys. Lett.* **901-3**, 194101, 2007.

The physiologic noise correlation by use of elastography

Sonogram



Wavelength tomography



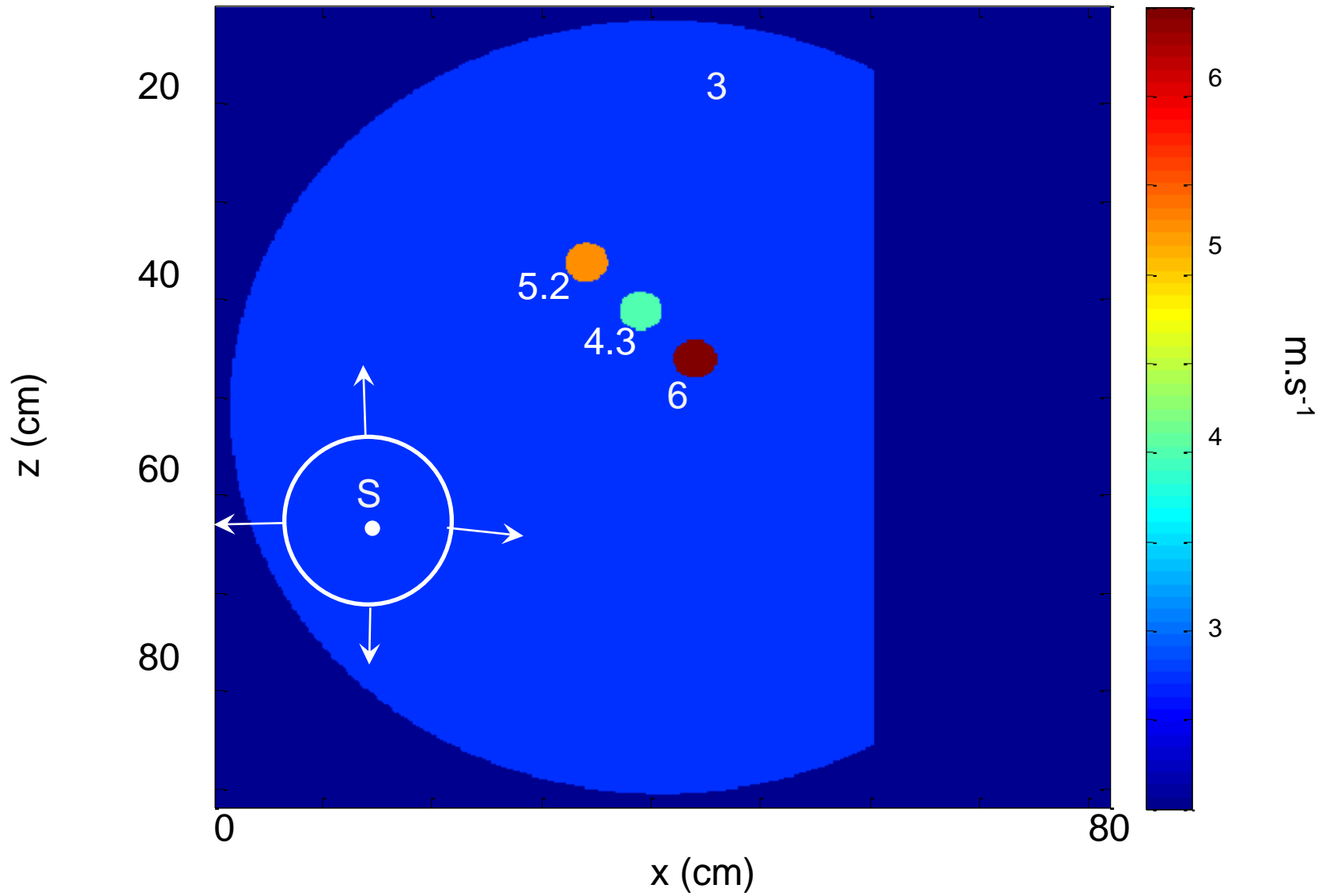
T. Gallot, S. Catheline, P.Roux, J.Brum, N.Benech, C.Negreira « Passive elastography: shear wave tomography from physiological noise correlation in soft tissues » IEEE transaction on UFFC, Vol.58 N°6, June 2011.

Shear wave imaging with a conventional scanner: the passive elastography approach

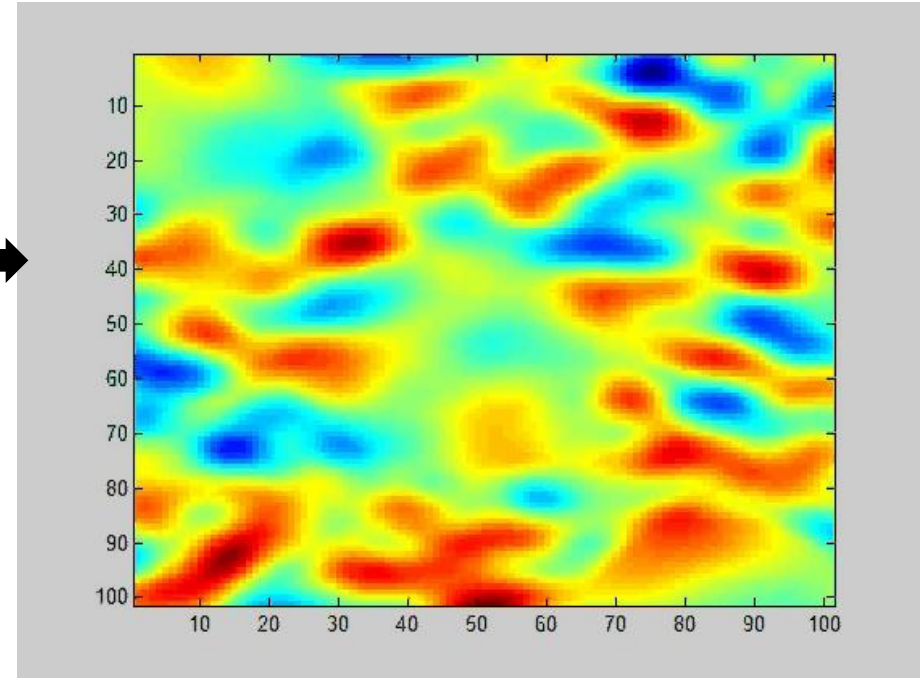
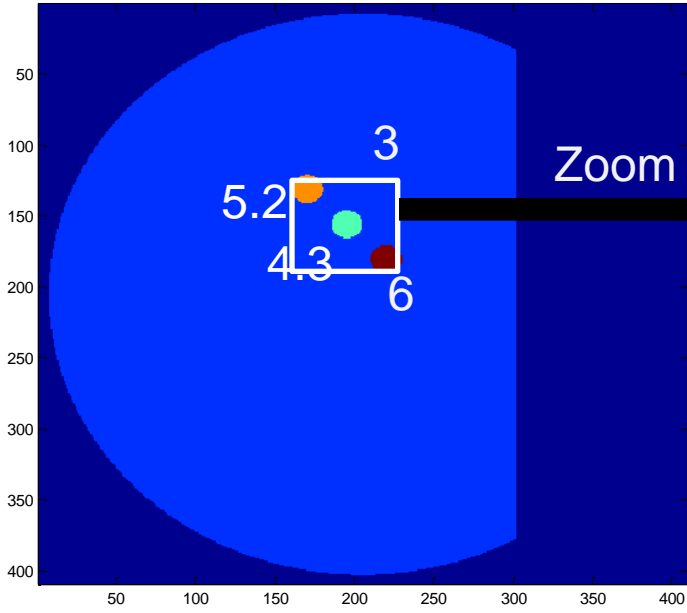
S.Catheline, R.Souchon, A. Hoang-Dinh and J-Y Chapelon

INSERM U1032, LabTAU, University of Lyon

The diffuse field approach: finite difference



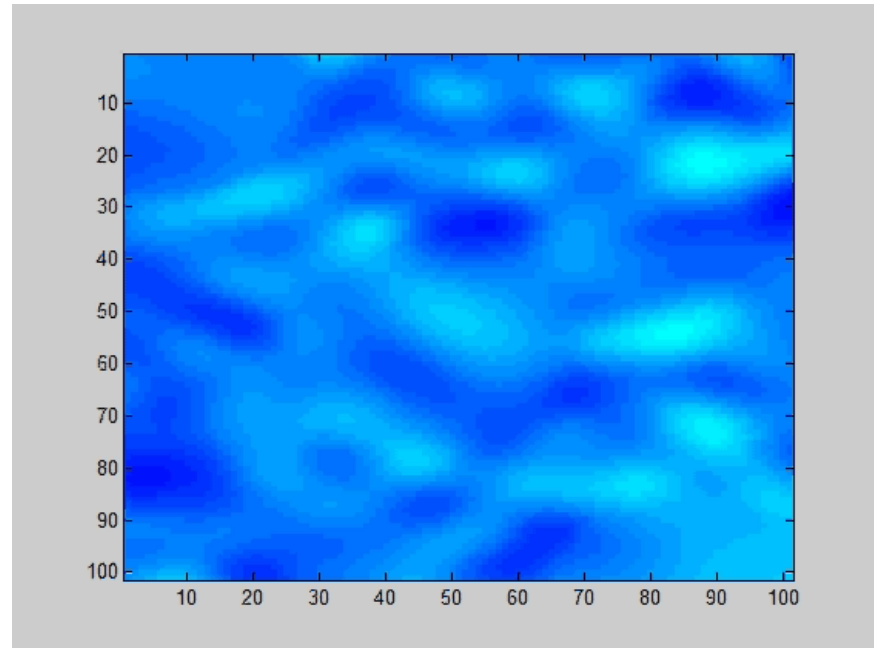
The diffuse field approach



Time reversal

Key for speed extraction=TR

TR=spatio-temporal
correlation (coda wave
interferometry)



S.Catheline, N. Benech, X. Brum, and C. Negreira, *Phys.Rev.Letter.* **100**, 064301 (2008).

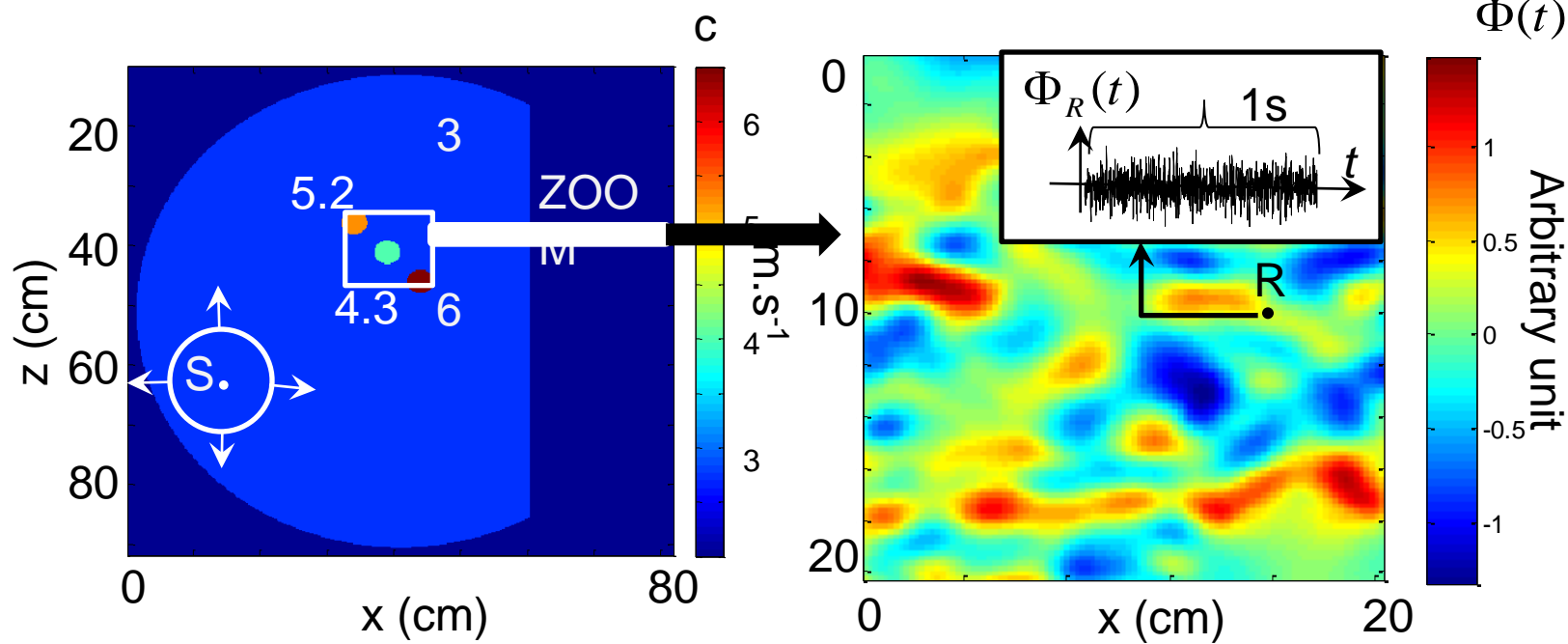
T.Gallot, S. Catheline, P. Roux, J. Brum, N. Benech, C. Negreira, *IEEE UFFC*, vol.58,6,p.1122 (2011)

$$\Delta\Phi - \frac{1}{c^2} \frac{\partial^2 \Phi}{\partial t^2} = 0 \rightarrow \psi^{RT} = \Phi(\vec{r}, t) \otimes \Phi(\vec{r}_0 - t) = \int \Phi \Phi^* dt$$

$$\varepsilon_z = \frac{\partial \Phi}{\partial z} \rightarrow \Delta \varepsilon_z - \frac{1}{c^2} \frac{\partial^2 \varepsilon_z}{\partial t^2} = 0 \rightarrow \xi^{RT} = \int \varepsilon_z \varepsilon_z^* dt \xrightarrow{\text{Plane wave}} \xi^{RT} \approx -k^2 \psi^{RT}$$

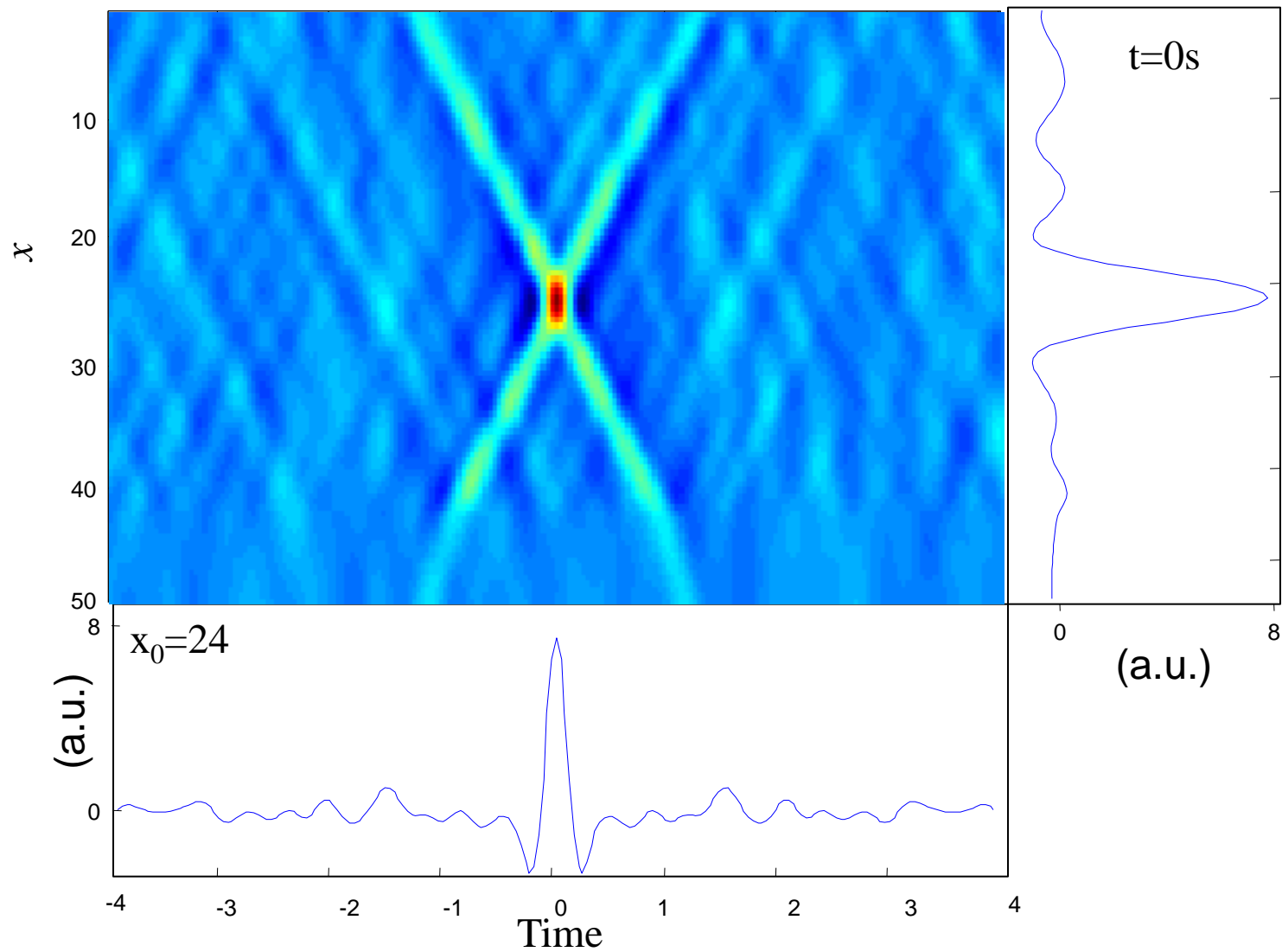
$$v = \frac{\partial \Phi}{\partial t} \rightarrow \Delta v - \frac{1}{c^2} \frac{\partial^2 v}{\partial t^2} = 0 \rightarrow V^{RT} = \int v v^* dt \rightarrow V^{RT} \approx -\omega^2 \psi^{RT}$$

$$c = \frac{\omega}{k} = \sqrt{\frac{V^{RT}}{\xi^{RT}}}$$

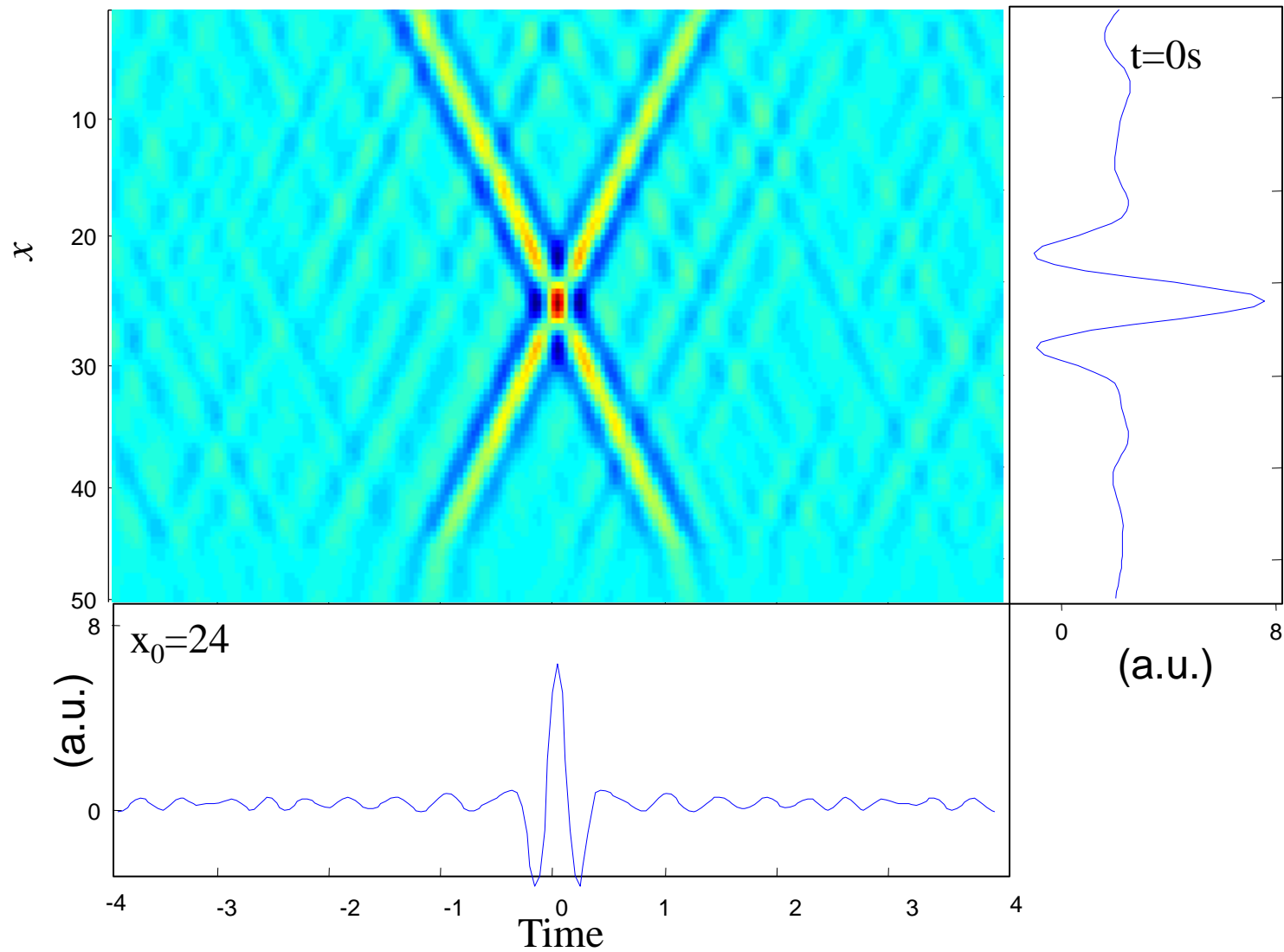


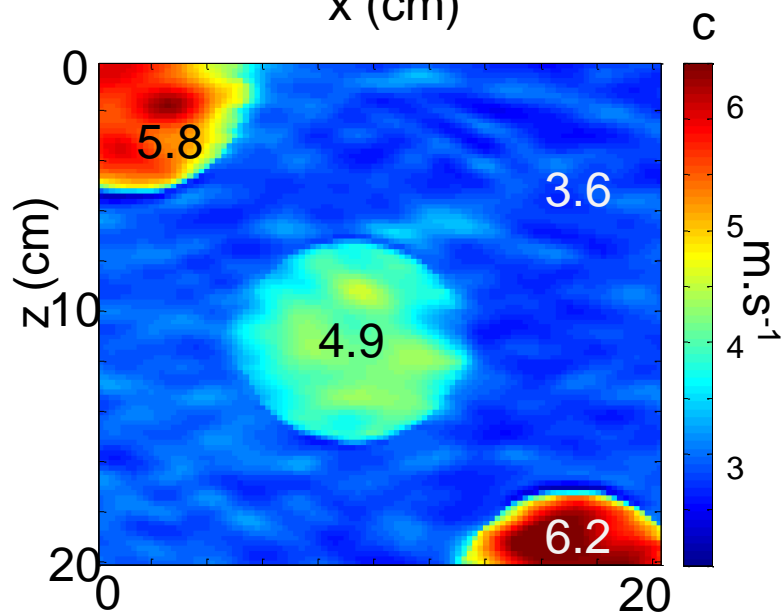
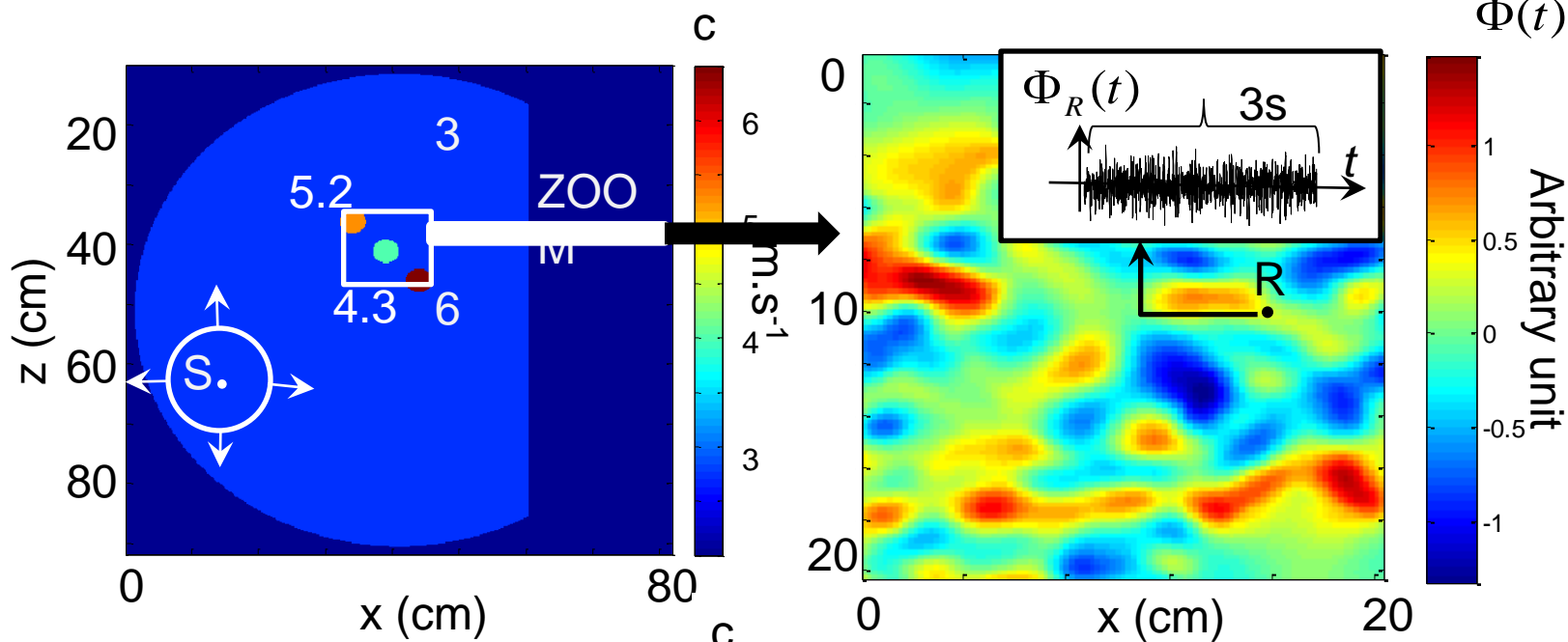
$F_{\text{sampling}} = 1000\text{Hz}$

Over sampling

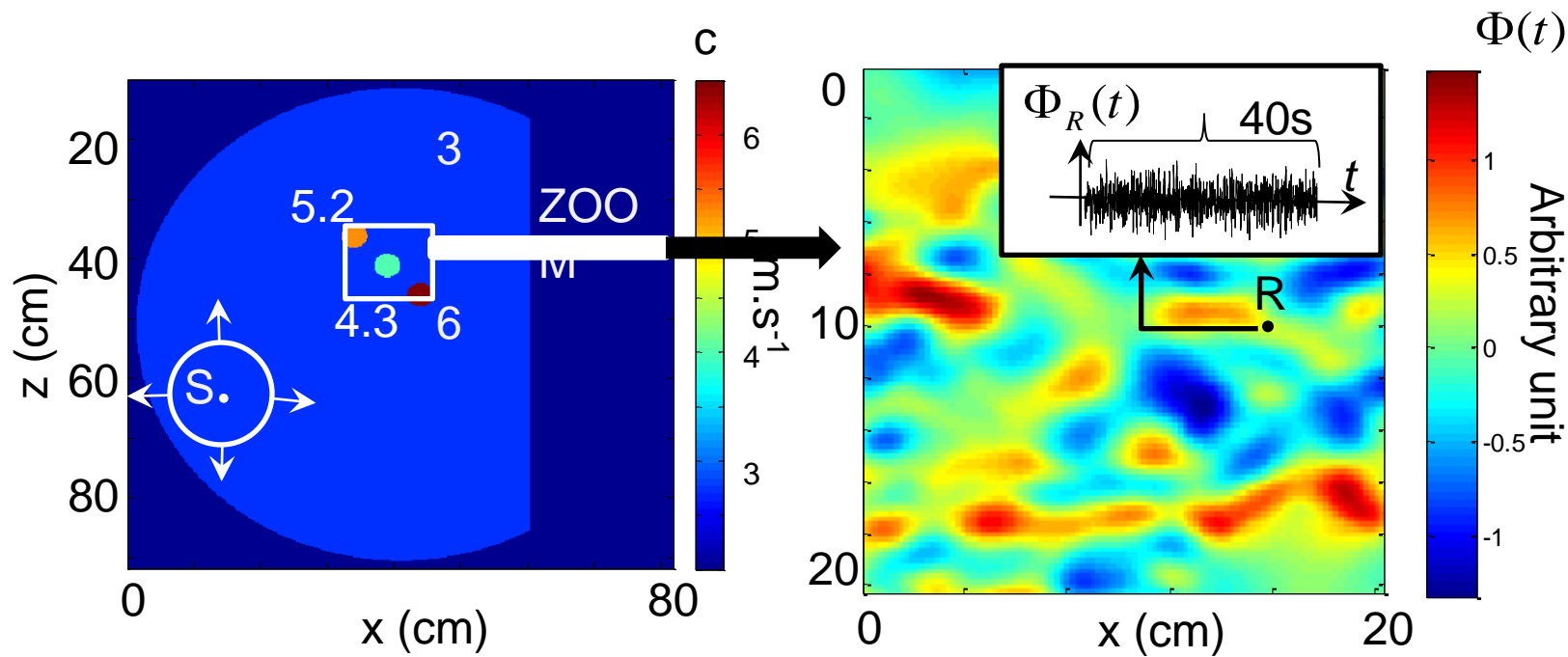


Over sampling



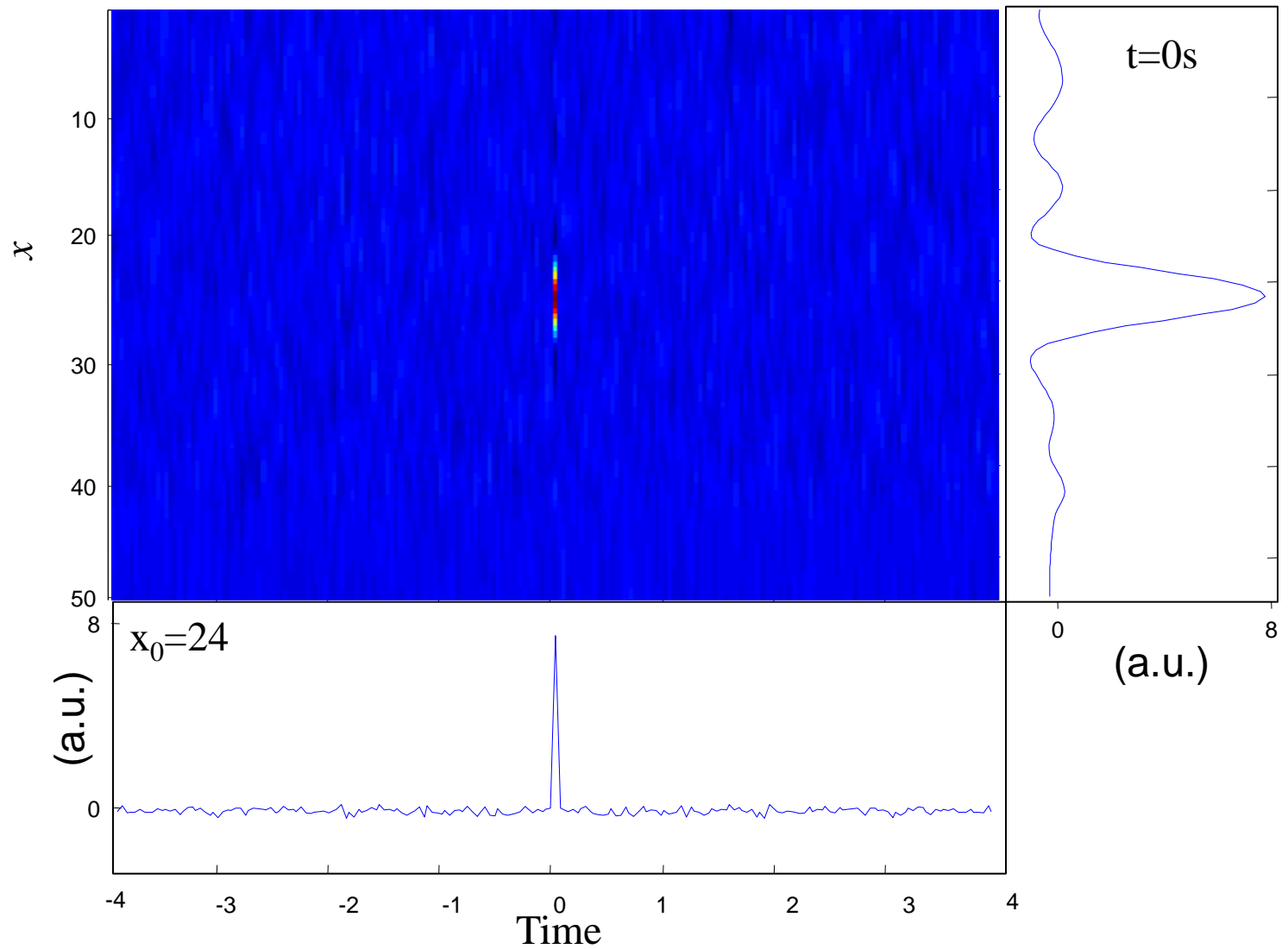


$$c = \frac{\omega}{\text{Re}(k)} = \sqrt{\frac{V^{RT}}{\xi^{RT}}}$$



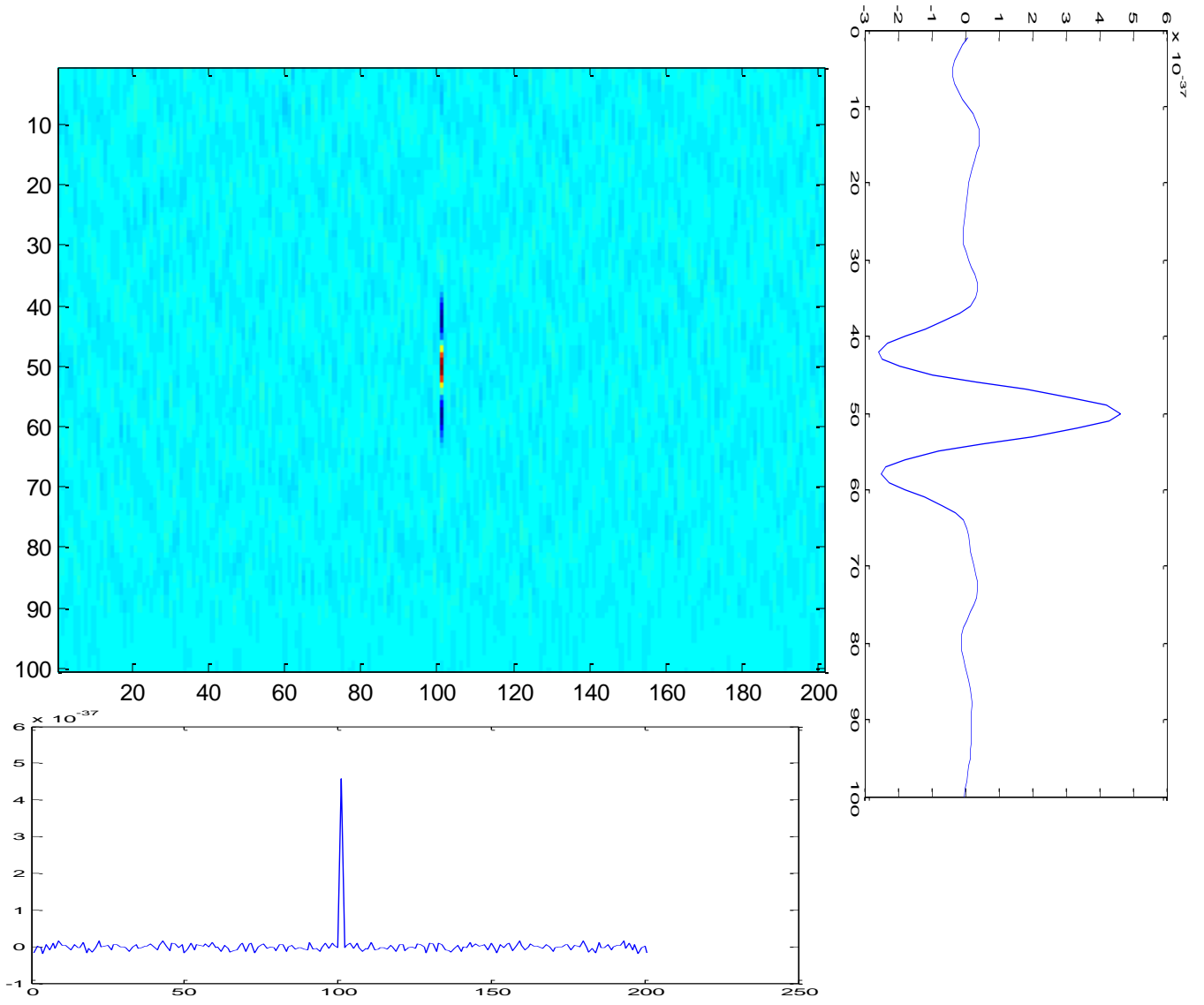
$F_{\text{sampling}}=25\text{Hz}$

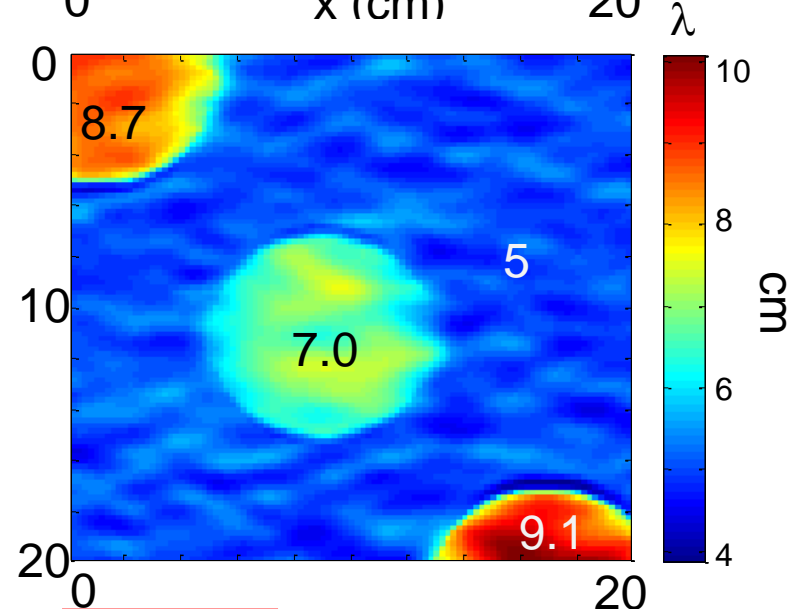
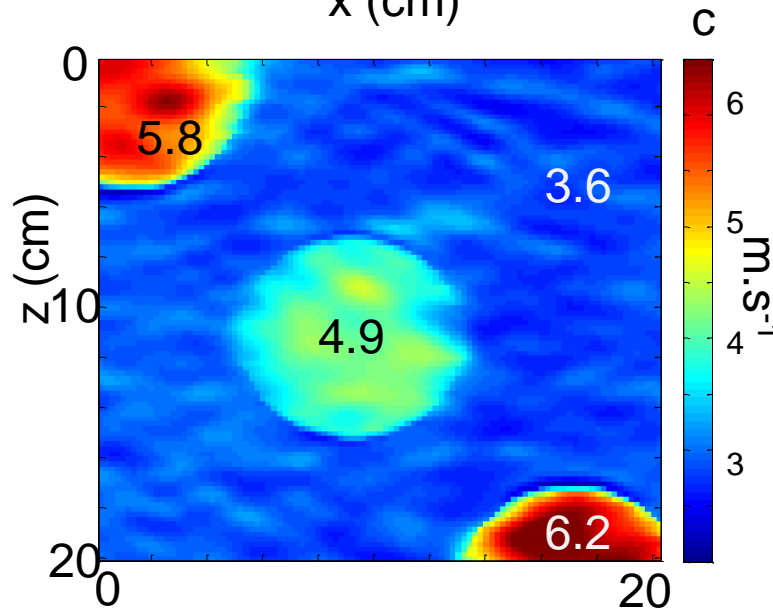
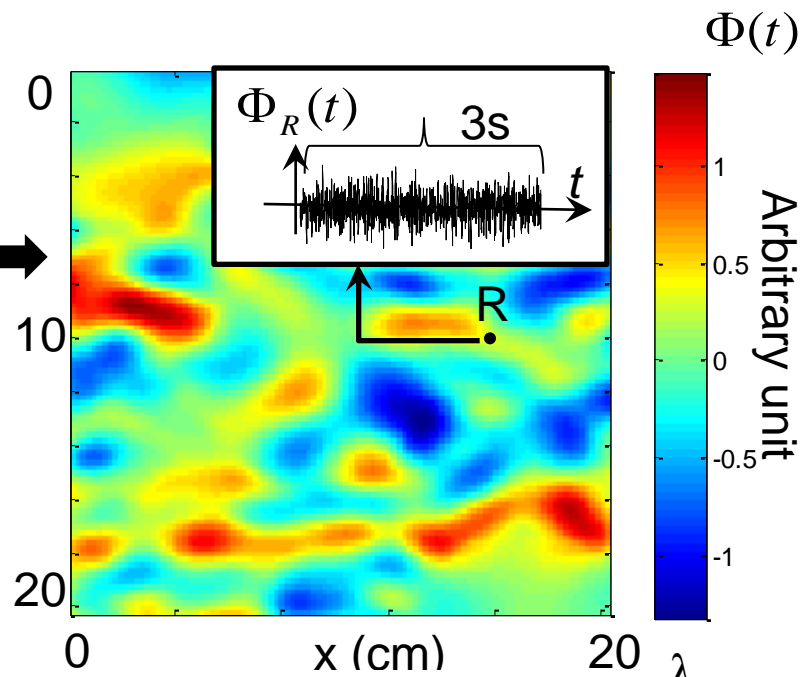
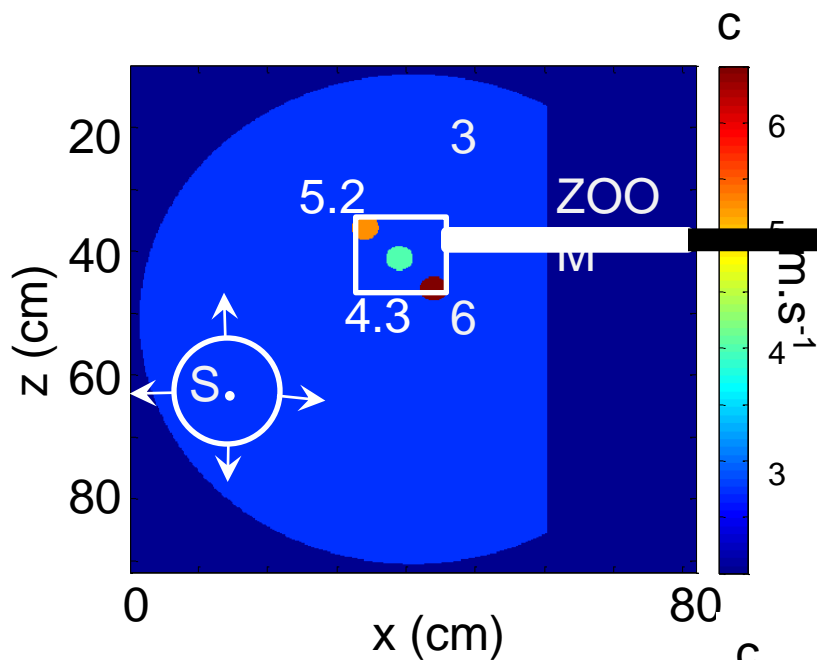
Under sampling



$$C(\vec{r}_0, \vec{r}; 0) = \int_0^T \psi_z(\vec{r}_0, \tau) \cdot \psi_z(\vec{r}, \tau) d\tau.$$

$$C_\phi(\vec{r}_0, \vec{r}; 0) = \int_0^T \psi_z(\vec{r}_0, \phi(\tau)) \cdot \psi_z(\vec{r}, \phi(\tau)) d\tau.$$



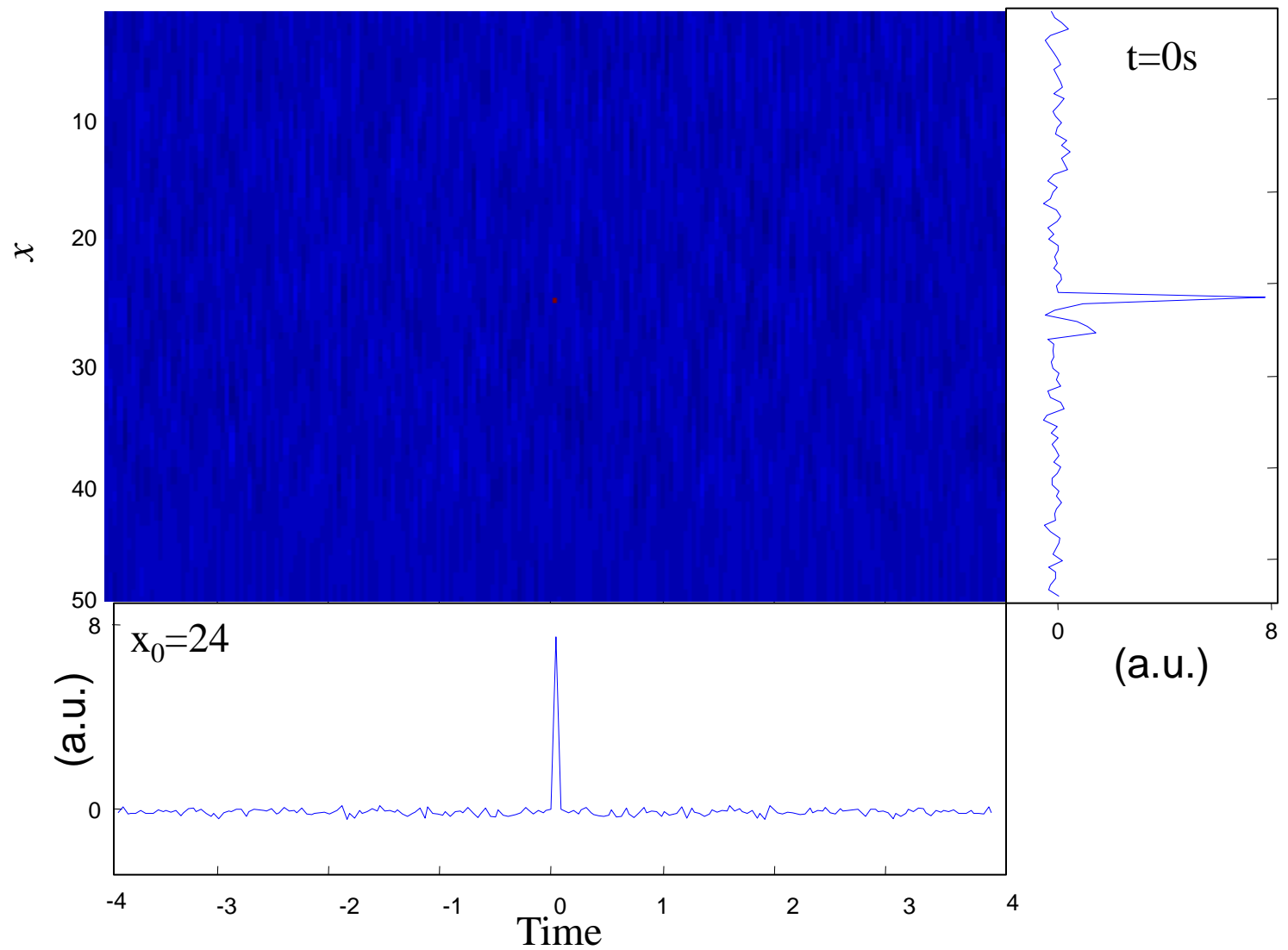


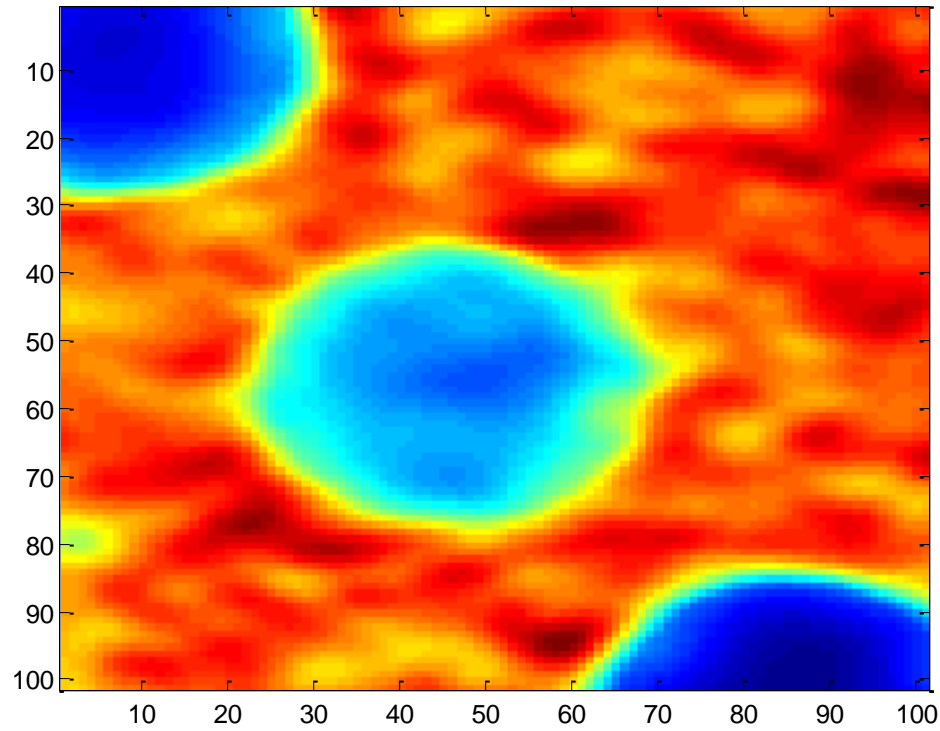
$$c = \frac{\omega}{\text{Re}(k)} = \sqrt{\frac{V^{RT}}{\xi^{RT}}}$$

$$k = \sqrt{\frac{\xi^{RT}}{\psi^{RT}}}$$

Infos spatiales uniquement
Pas d'info temporelle

Elasticity imaging: under sampling experiments





$$\text{Im}[G_{mn}(\mathbf{0}, \mathbf{r})] = \frac{k}{12\pi\mu} \left\{ \left[\left(\frac{\beta}{\alpha} \right)^3 (j_0(qr) + j_2(qr)) + 2j_0(kr) - j_2(kr) \right] \delta_{mn} + \left[3j_2(kr) - 3 \left(\frac{\beta}{\alpha} \right)^3 j_2(qr) \right] \gamma_m \gamma_n \right\}$$

$$\text{Im}[G_{mn}(0,0)] = \frac{k}{12\pi\mu} \left[\left(\frac{\beta}{\alpha} \right)^3 + 2 \right] \cong \frac{k}{6\pi\mu} = \frac{f}{3\rho c_s^3}$$

The softer, the higher the amplitude

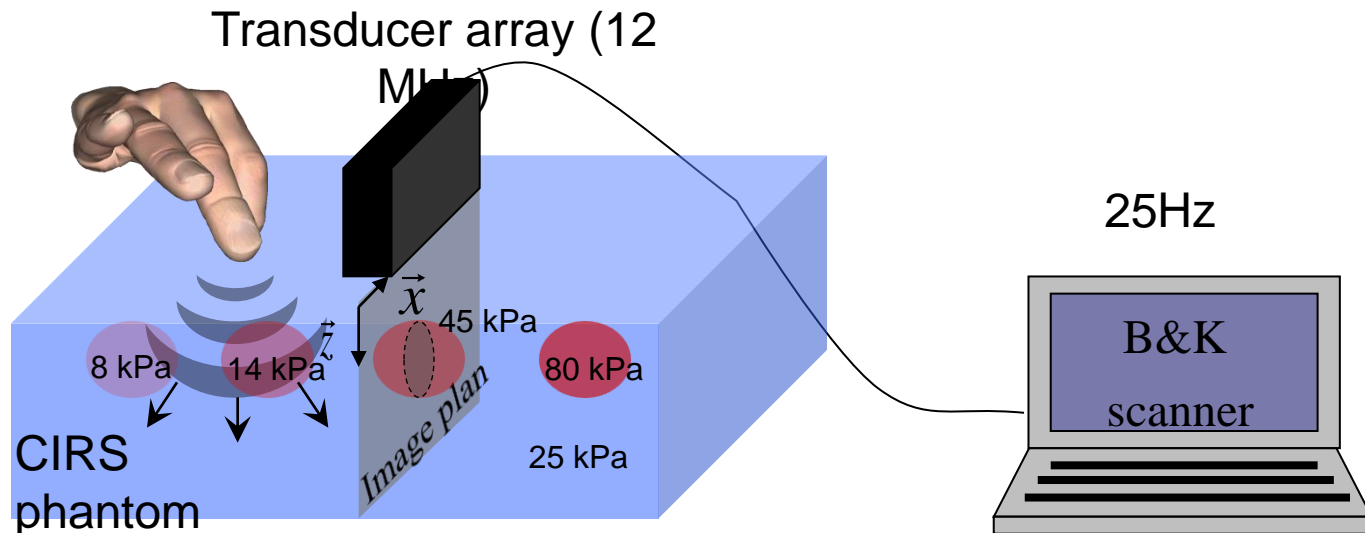
Is it always true? Not sure. Bar, plate, string

$$G^{plate}(0, x) = \frac{ic^2}{8\omega^2} [j_0(kr) + N_0(kr) - j_0(i\gamma r) - iN_0(i\gamma r)]$$

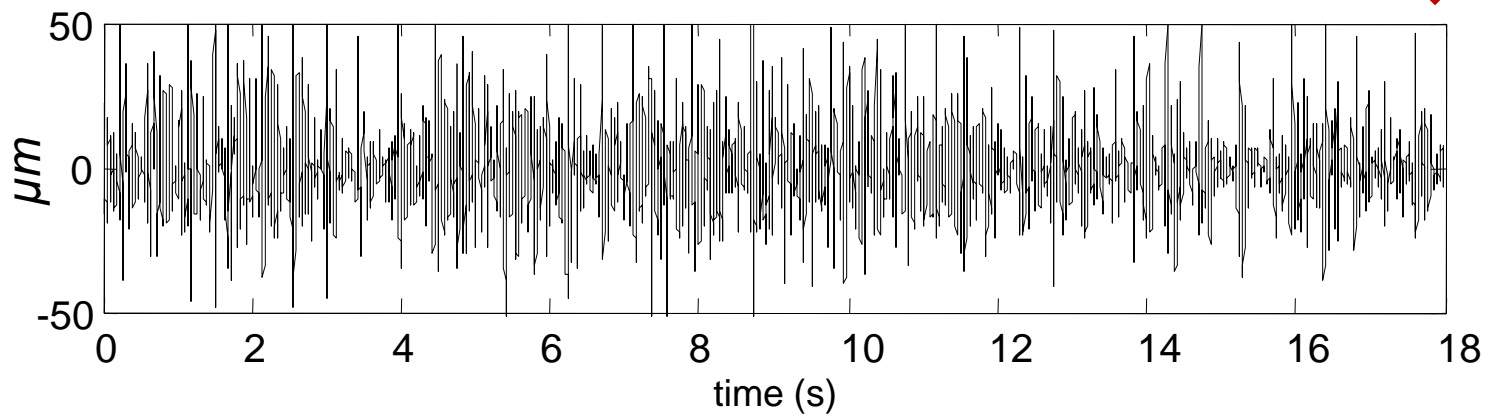
$$G^{bar}(0, x) = \frac{ic^3}{4\omega^3} e^{ikx}$$

$$G^{string}(0, x) = i \frac{c}{2\omega} e^{ikx}$$

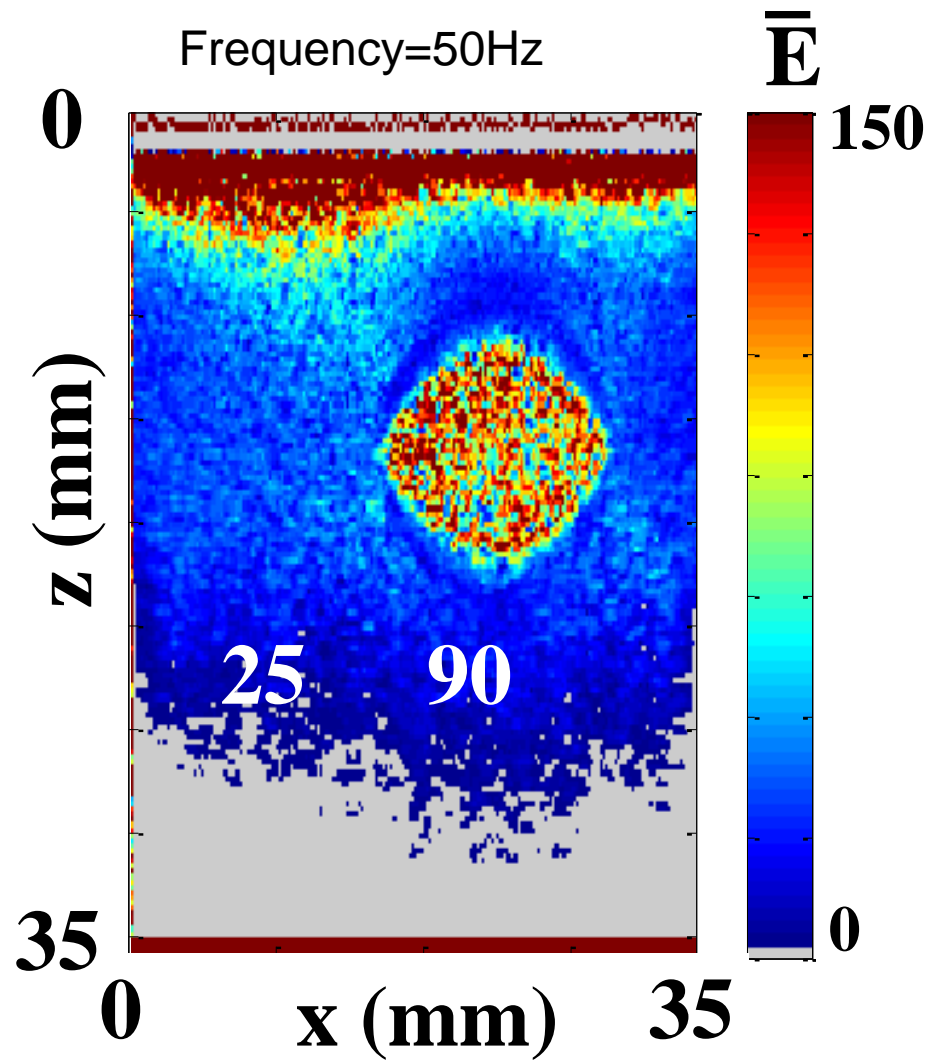
Phantom experiment



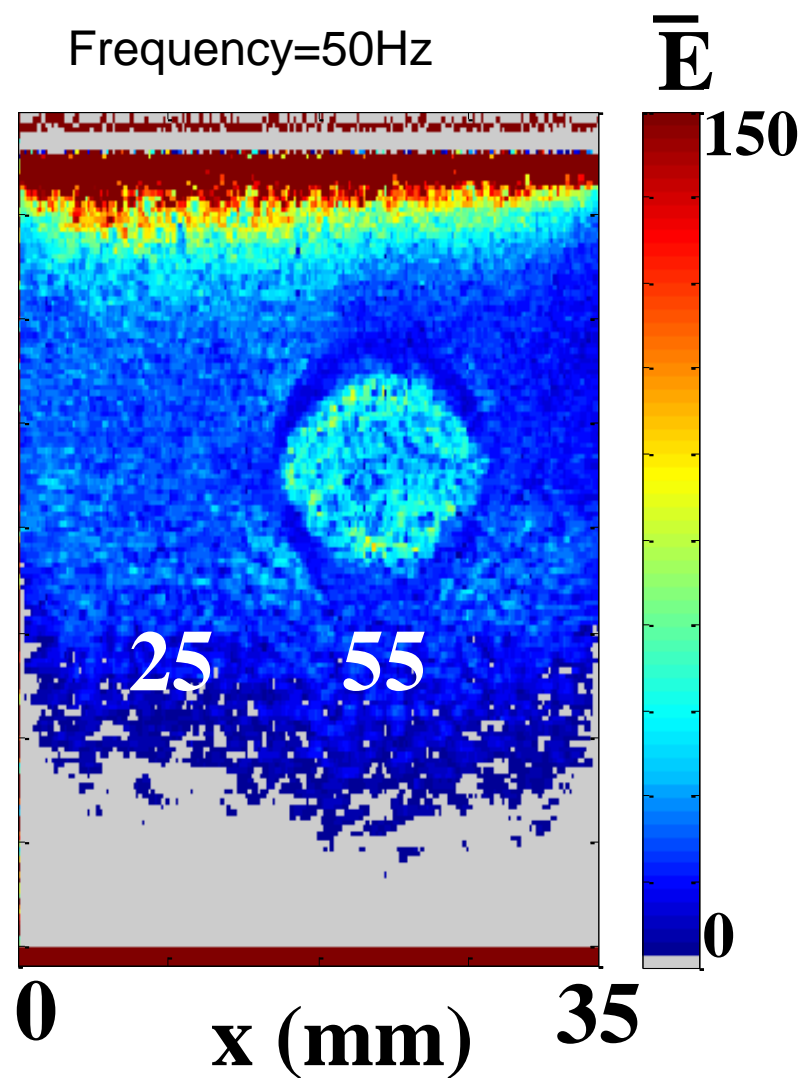
$$\Psi_z(x,z;t)$$



Phantom experiment

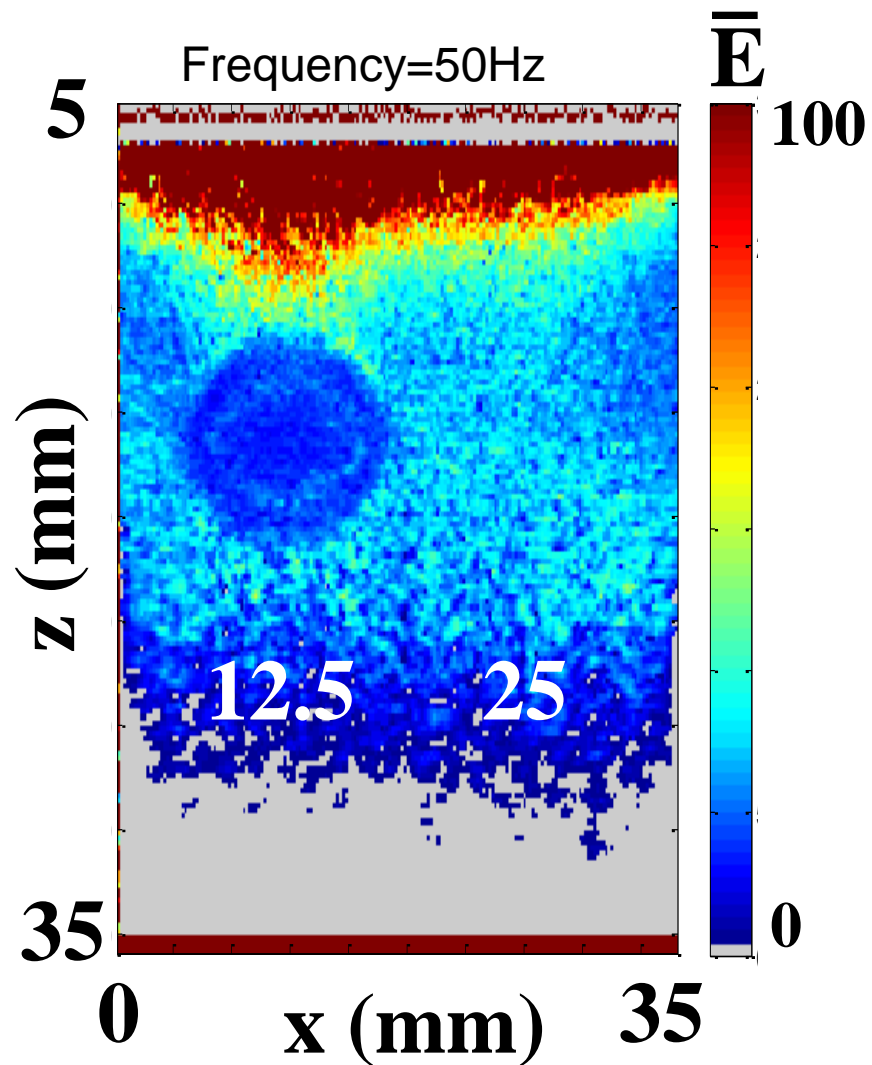


Constructor: 80kPa

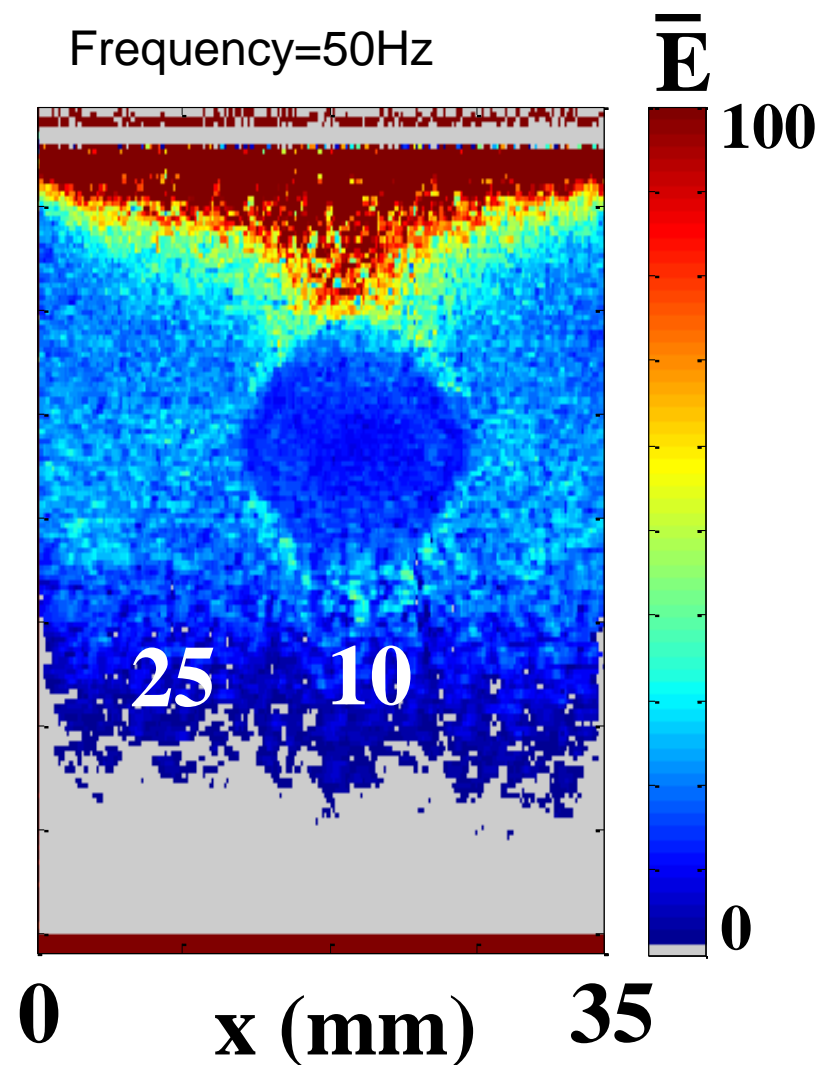


Constructor: 45kPa

Phantom experiment



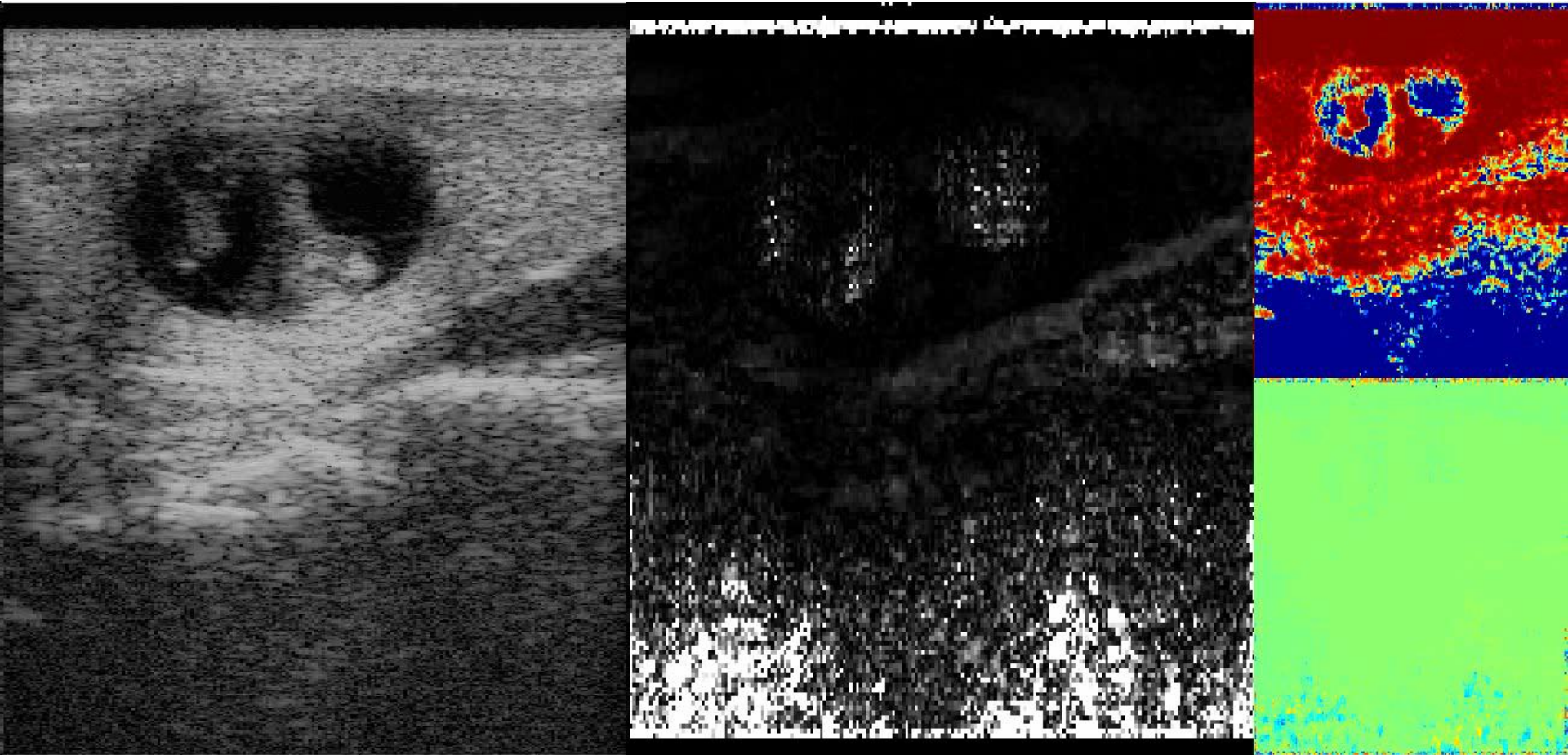
Constructor: 14kPa



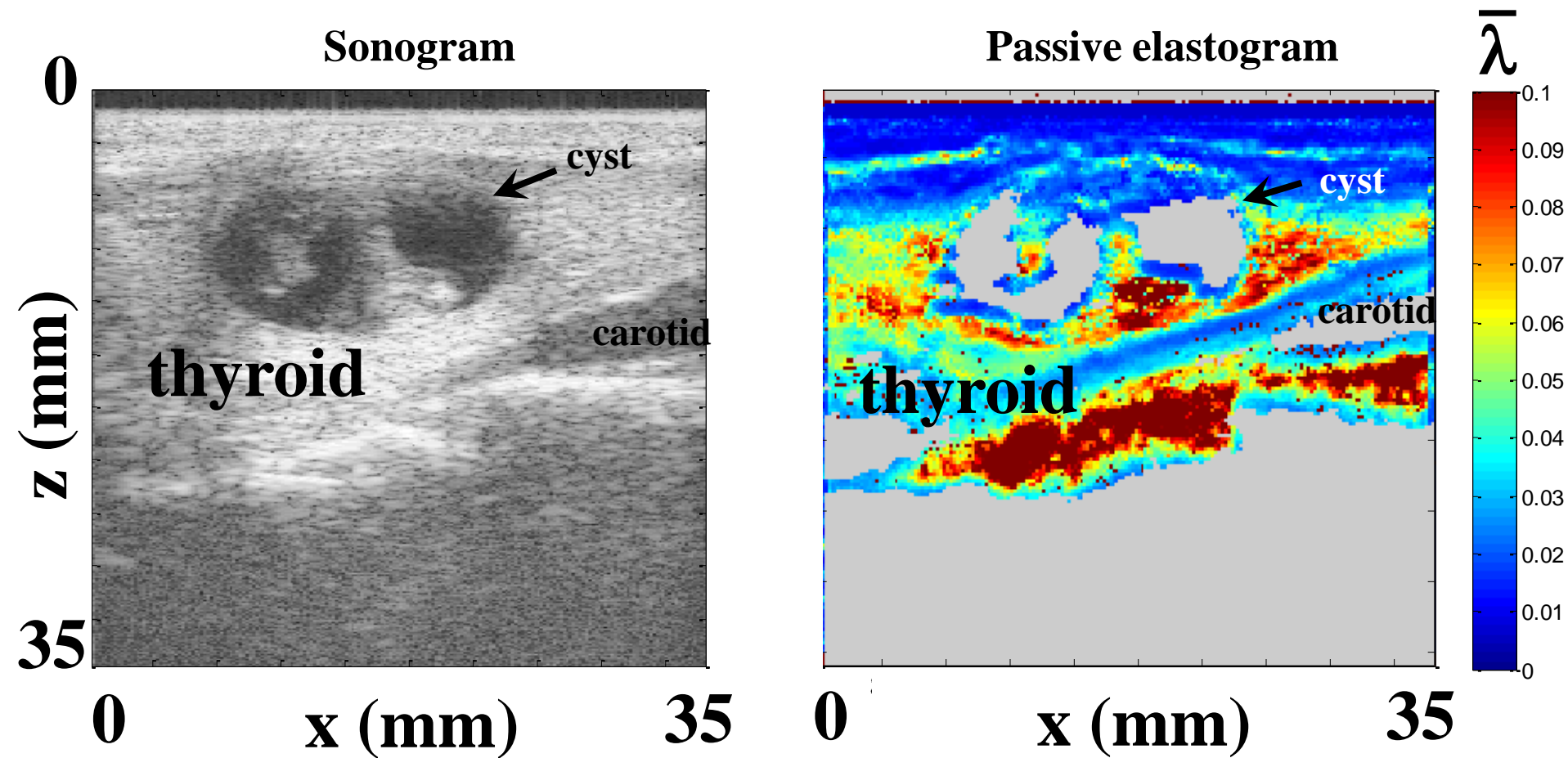
Constructor: 8kPa

Preliminary *in-vivo*

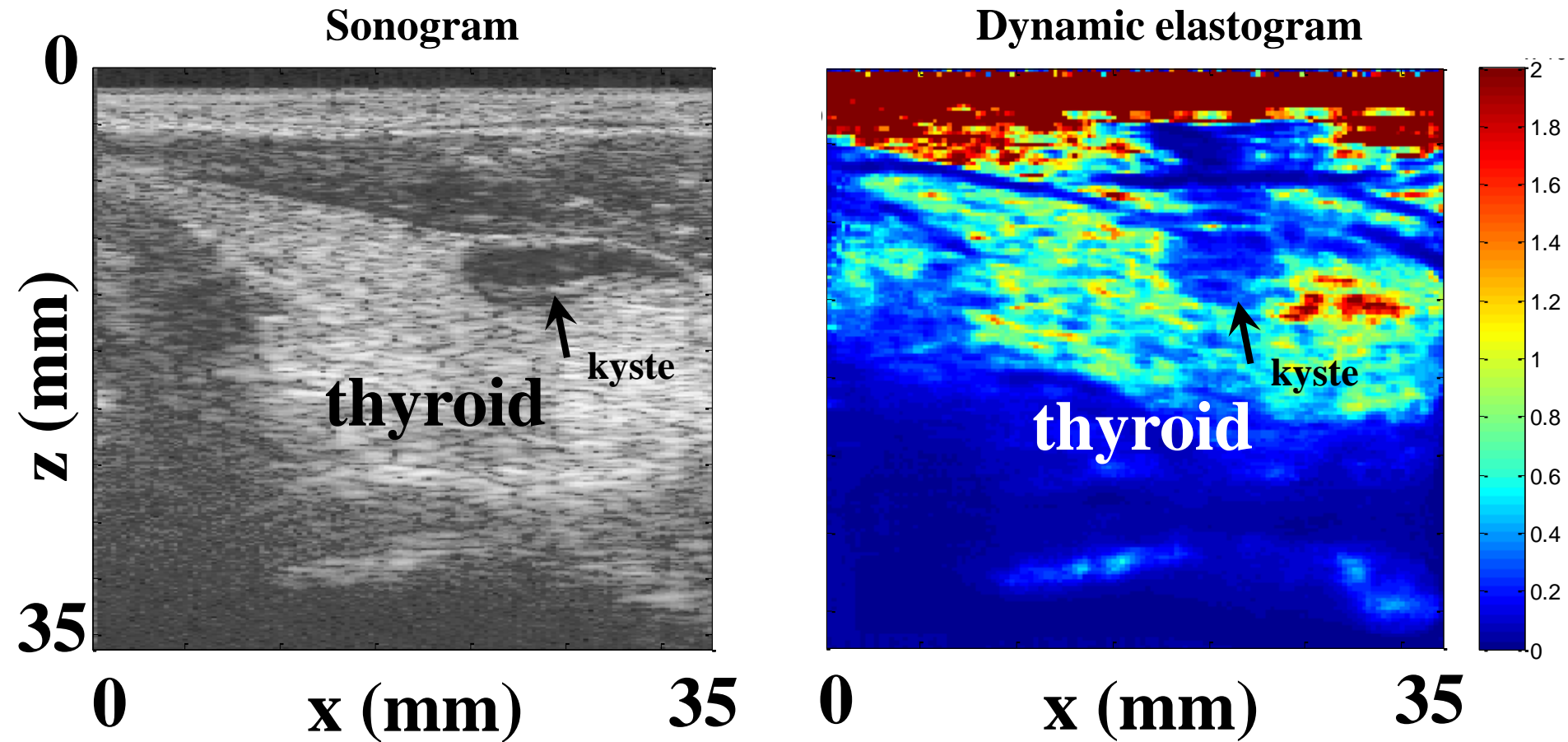




800 images @ 25Hz



$$k = \sqrt{\frac{\xi^{RT}}{\psi^{RT}}}$$



Milieux elastique, homogène,
isotrope, linéaire

$$(\lambda + 2\mu) \overrightarrow{\text{grad}} \text{div}(\vec{u}) - \mu \overrightarrow{\text{rot}} \overrightarrow{\text{rot}} \vec{u} - \rho \frac{\partial^2 \vec{u}}{\partial t^2} = \vec{0}$$

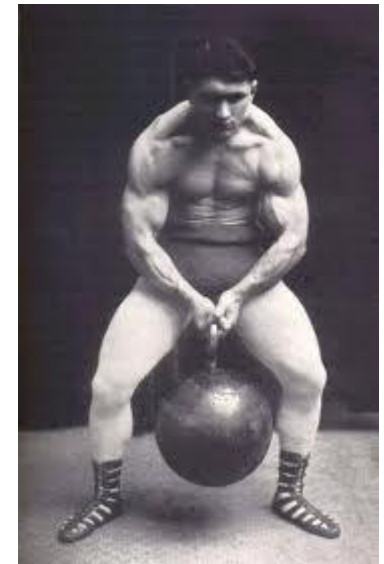
$$C_P = \sqrt{\frac{\lambda + 2\mu}{\rho}} \approx \sqrt{\frac{\lambda}{\rho}} \quad C_S = \sqrt{\frac{\mu}{\rho}}$$

Soft tissues:

$$\lambda = 2,5 \text{ GPa}$$

$$\mu = 25 \text{ kPa} \ll \lambda$$

$$\sigma = \frac{Mg}{S} = \frac{130 \cdot 10}{10^{-4}} = 0.013 \text{ GPa}$$



Manual palpation reveals shear elasticity μ